VISCOELASTIC TRANSITION OF LUBRICANTS

A THESIS

Presented to

The Faculty of the Division of Graduate Studies

By

Vijay Kumar Khemka

In Partial Fulfillment

of the Requirements for the Degree

Master of Science in Mechanical Engineering

Georgia Institute of Technology

January, 1978

VISCOELASTIC TRANSITION OF LUBRICANTS

Approved:

Ward O. Winer, Chairman

John T. Berry

Donald C. O'Shea

Date approved by Chairman: 9 February 1978

ACKNOWLEDGMENTS

The author wishes to thank the members of his reading committee for their time, interest and suggestions. The advice and assistance of the committee chairman, Professor Ward O. Winer, is particularly appreciated.

The author is thankful to Mr. Scott Bair and Mr. Gene Clopton for their assistance and valuable suggestions.

The author also wishes to thank Mr. and Mrs. Kiran Fatehpuria for their support and encouragement.

Finally, particular thanks are due to my wife, Uma Khemka for helping in many tangible and many more intangible ways.

The research reported herein was supported by NASA Grant NSG 3106. This support is gratefully appreciated.

TABLE OF CONTENTS

TABLE OF CONTENTS (Continued)

LIST OF TABLES

LIST OF ILLUSTRATIONS

LIST OF ILLUSTRATIONS (Continued)

LIST OF ILLUSTRATIONS (Continued)

NOMENCLATURE

A' = Area of Sample

A_l = Linear Acceleration

C = Rate of Cooling

C_p = Specific Heat

E_A = Peak to Peak Value of Acceleration Signal

E_f = Peak to Peak Value of Force Signal

F = Total Force

G' = Storage Modulus

G'' = Loss Modulus

K = A Constant defined as $\frac{S_{Af}}{S_{AA}}xb$

L = Length of Sample

M = Torque

P_V = Viscoelastic Transition Pressure

R = Radius of Sample

R_1 = Radius of Inner Cylinder

R_2 = Radius of Outer Cylinder

S_{AA} = Charge Amplifier Sensitivity for Acceleration

S_{Af} = Charge Amplifier Sensitivity for Force

S_{OA} = Oscilloscope Sensitivity for Acceleration

S_{Of} = Oscilloscope Sensitivity for Force

T = Temperature

T_v = Viscoelastic Transition Temperature

X_l = Linear Displacement

b	=	Form Factor
f	=	Force applied by the Liquid
f_e	=	Elastic Force
f_v	=	Viscous Force
g	=	Acceleration due to Gravity
h	=	Thickness of Sample
t	=	Time
α	=	Angular Displacement
β	=	Isothermal Compressibility
γ	=	Strain
γ_o	=	Strain Amplitude
δ	=	Phase Angle between Force and Displacement
ϵ'	=	Permittivity
ϵ''	=	Loss Tangent
θ	=	Phase Angle between F and X_1
θ'	=	Angle between Cone and Plate
ν	=	Linear Frequency
σ	=	Stress
σ_o	=	Stress Amplitude
τ_M	=	Mechanical Relaxation Time
τ_D	=	Dielectric Relaxation Time
ω	=	Circular Frequency

SUMMARY

This thesis reports the viscoelastic transition temperature as a function of frequency for seven lubricants (polyphenyl ether, cycloaliphatic hydrocarbon, naphthenic base oil, naphthenic base oil blended with 4.0 percent high molecular weight polymer, cycloaliphatic hydrocarbon traction fluid with additive, tri-aryl phosphate and perfluorinated polymer) at atmospheric pressure as measured by shear mechanical relaxation technique. An experimental technique was devised whereby the data necessary to determine viscoelastic transition temperature of a lubricant under shear may be obtained using only an impedance head with shaker, a signal generator with amplifiers and an oscilloscope. The plot of real part of shear modulus as a function of temperature and frequency allows the determination of the viscoelastic transition temperature. The frequency range covered was 100 to 1000 Hz and the temperature range varied from 25 to -80 C.

Results obtained from shear mechanical relaxation were compared with those obtained from dilatometry and dielectric measurements. The data indicated that the viscoelastic transition temperature increased with increasing frequency at a rate which ranged from 4.25 to 8.5 C per decade in frequency. Viscoelastic transition temperature was found to be higher and relaxation time was found to be longer for shear mechanical relaxation than those obtained from dielectric measurement for all the fluids studied except perfluorinated polymer for which the case was reverse.

Because of the shearing nature of the lubricant deformation in elastohydrodynamic lubrication, the shear mechanical relaxation may be more relevant for this application than other methods of determining viscoelastic transition. Moreover, many workers in the field of elastohydrodynamic lubrication assume that the lubricant in EHD contacts remains in the viscous liquid state. Adjustment to the existing theory will be necessary if the physical state of a lubricating oil in an EHD contact indicates that it falls in or near the glassy state. In that case, the solid-like properties of the lubricant will be the controlling material characteristics.

CHAPTER I

INTRODUCTION

A. Need for Study of Tribology and Rheology

Tribology has been defined as the science and technology of interacting surfaces in relative motion [1]. The science of tribology plays a vital role in our advanced technological society. The loss of energy due to friction is very high. A conservative estimate [2] reveals that about one-third to one-half of the total production of energy in the world is lost due to friction. Wear causes changes in dimensions and eventual breakdown of the machine element and the entire machine.

Several reasons for studying tribology are: reducing the waste of the world's energy, conserving critical natural resources, maintaining production schedules in a plant, and increasing the effective service life of machines.

Tribology is concerned with the entire realm of interacting surfaces in relative motion and as such, is interdisciplinary, requiring attention from virtually all branches of science.

Jost [3], through a systematic study and implementation of tribological principles, quoted a possible savings of $1.24 billion per annum for the United Kingdom in 1966. In a recent article, Jost [4] claims potential annual savings of $12 to $16 billion for the United States.

Several fatal failures and disasters caused by failure of

mechanical equipment have been traced to tribological problems. Mechanical equipment reliability [5] is also an important concern in part dependent on tribology.

Lubrication problems of today are complicated because of the severe operating conditions to which many systems are subjected. There are many machine elements in which contacting surfaces do not conform to each other and the full burden of the load must be carried by a very small area of contact. This is unlike hydrodynamic lubrication where the surfaces conform to each other so that the load is supported by a relatively larger area. Some examples of there non-conforming surfaces are: mating gear teeth, cam and followers, and rolling element bearings. The ball and race in a ball bearing conform to some degree in one direction, but to a very little extent in the other direction. There were doubts until the 1950's that these nonconforming surfaces with extremely small area of contact could be separated by an oil film. The lubrication of these non-conforming surfaces is referred to as elastohydrodynamic lubrication [6,7].

A thorough understanding of lubricant rheology in an EHD contact is still lacking [8]. The viscoelastic transition of lubricants, and therefore the rheological behavior in the glassy state, plays a significant role in determining the rheological behavior of lubricants in EHD lubrication.

B. Elastohydrodynamic Lubrication

Elastohydrodynamic lubrication (EHD) refers to lubrication. Situations in which elastic deformation of the surrounding plays a

significant role in the hydrodynamic lubrication process. The mechanism of elastohydrodynamic lubrication is essentially an extension of ordinary hydrodynamic lubrication which was described by Osborne Reynolds in 1996 in his masterpiece work [9].

Elastohydrodynamic lubrication deals with nonconforming surfaces that are elastically deformed by loads which must be carried over small areas. The load gives rise to a pressure which is distributed over the small contact area. Typical maximum pressure found in bearings and gear contacts is of the order of 1.4 to 3.5 GPa. Such nonconforming surfaces may be represented by a sphere or cylinder loaded against a flat surface where the load causes the surfaces to elastically deform over a small region.

Sliding is defined as the difference in speed between the bearing surfaces, while rolling is referred to the average speed of the bearing surfaces. An EHD contact can move by rolling, by sliding or a combination of the two. Sliding generates frictional heat and imposes large shear forces on the lubricant film. These films are usually only a few micro inches thick in the contact area. For such a thin film to permit relative motion of the surfaces, it must undergo shearing at a very high rate.

The conjunction zone of a typical EHD contact can be divided into three general regions: the inlet region, the Hertzian region, and the outlet region. The pressure and temperature in the contact build up gradually over the inlet region to high values in the Hertzian region. The pressure has a spike before dropping sharply to zero at the outlet region. Therefore, the properties of the lubricant, while passing through

these regions, change within a matter of milliseconds. The properties in each region are determined by the temperature, pressure and relaxation time that exist in each region. The physical state of the lubricant is important to investigate. Since the behaviors of the lubricant, as governed by pressure and temperature conditions within the inlet region, influence the film thickness, this film thickness is controlled by the rate at which the lubricant is drawn into the conjunction zone and by the viscosity of the lubricant in the inlet region. The lubricant behavior in the hertzian zone is important primarily in determining sliding friction or traction. The simultaneous existence of extremes of high pressure and temperature in this lubricant films and short residence times make the elastohydrodynamic contact a most unusual physical system. The hertzian condition of contact is a dominating feature of EHD lubrication, because it establishes the overall shape of the contacting surfaces.

C. Viscoelastic Transition Temperature and Glassy State

Viscoelastic transition is characterized by certain experimental observations which occur while the imposed environment of the material is changing. Commonly experiments are performed for isobaric cooling or isothermal compression of the material. At the viscoelastic transition, many material properties change in a characteristic manner. As the temperature is reduced in the liquid region, the material contracts and the viscosity increases. If the material is capable of crystallization, a point will be reached where crystallization starts. If crystallization does not occur or can be avoided, the viscosity will continue to increase until some level of 10^{7} - 10^{12} Pas is reached [10,11,12]. At this point,

the material becomes rigid and the thermal expansion coefficient decreased to about one-half or one-third of its value in the melt or liquid state as shown in Figure 1.

Viscoelastic transition is also accompanied by a change in the specific heat, c_p, isothermal compressibility, β, and other secondary properties. It corresponds to a change in slope of a plot of specific volume versus temperature as shown in Figure 2. Thus, viscoelastic transition phenomena are a characteristic of any liquid which can be supercooled to a sufficiently low temperature without crystallization.

Viscoelastic transition phenomena are often referred to as an apparent second-order transition since it is characterized by a discontinuous change in the secondary thermodynamic quantities. These changes occur over a range of temperatures and are not strictly discontinuous. Ferry [13] and Howard [14] showed that viscoelastic transition phenomena are not true second-order thermodynamic transitions since at viscoelastic transition temperature, T_V, the substance is not in thermodynamic equilibrium. This is due to the slowness of molecular rearrangements at this temperature. This absence of thermodynamic equilibrium is part of the definition of the glassy state.

Below T_V, the degree of order will appear fixed and will not vary with temperature or pressure during the time of experimental observation. Because of this, the structural degrees of freedom are said to be frozen-in and therefore, the structural contribution to α, c_p and β are absent in the glassy state.

The effect of pressure on T_V is shown in Figure 2. The viscoelastic transition temperature shifts upward as the pressure is increased.

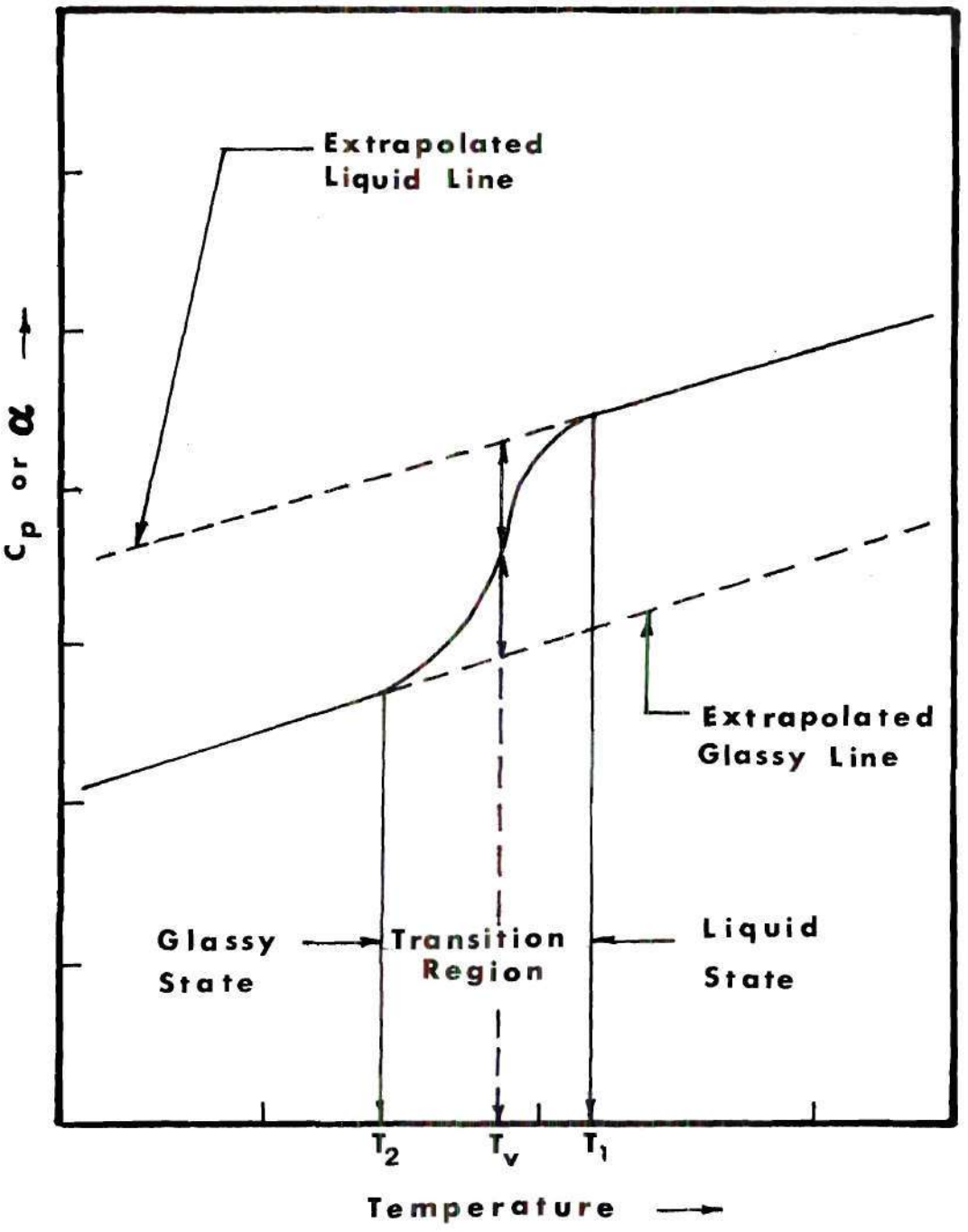

Figure 1. Thermal Expansion Coefficient or Specific Heat for a Typical Glassy Material [8].

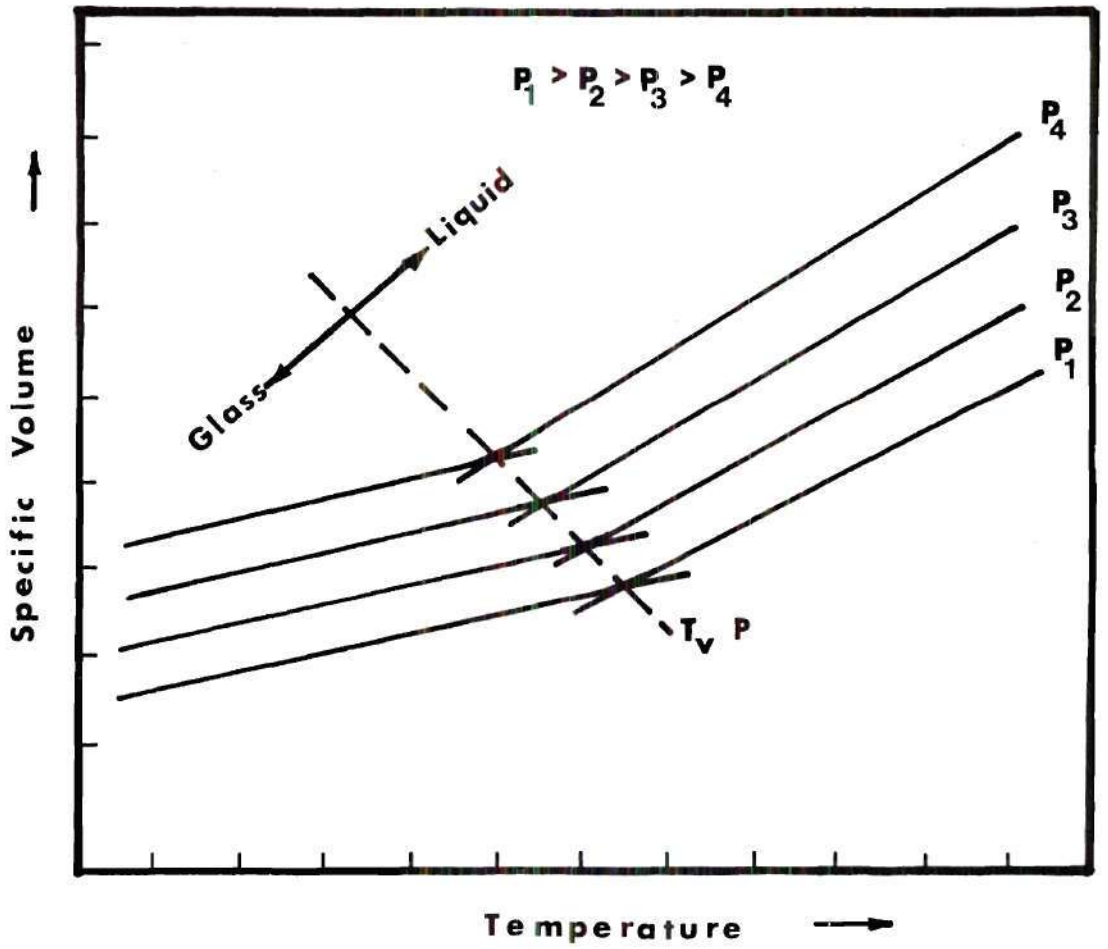

Figure 2. Typical Plot of Specific Volume Versus Temperature for a Glassy Material at Different Formation Pressures [8].

The increase in T_V with pressure will be sufficient to maintain an isoviscous state. A sufficiently high pressure can induce a transition from the liquid state to the glassy state without requiring a decrease in the temperature. Like pressure, viscoelastic transition temperature also increases as frequency is increased. The effect of frequency on T_V is shown in Figure 3.

The transition temperature of a material is a function of the imposed rate of change of the material's environment, and for a series of constant rate experiments, the transition temperature curve is a constant relaxation time curve. The characteristic time of the experiment is dependent on the observation time employed in the experiment. An approximate value of the relaxation time of the material when transition occurs is the observation time employed in the experiment. The range in the relaxation time of the material as it goes through the transition from liquid to glass is from 0.1 to 10^2 times the observation time. In the transition region the material exhibits both viscous and elastic behavior relative to the process. The range of transition region is indicated on Figures 1 and 2.

As a result of the non-equilibrium state, the thermodynamic history of a glass forming liquid has considerable influence on the structure, the transition, and the properties in the glassy state. The rate of the imposed environmental change effects the transition point and the properties of the glassy substance. Viscoelastic transition can be reached by isobaric cooling, isothermal compression, an imposed rate change or a combination of these. For example, the influence of the rate of cooling C, on the shift of the viscoelastic transition

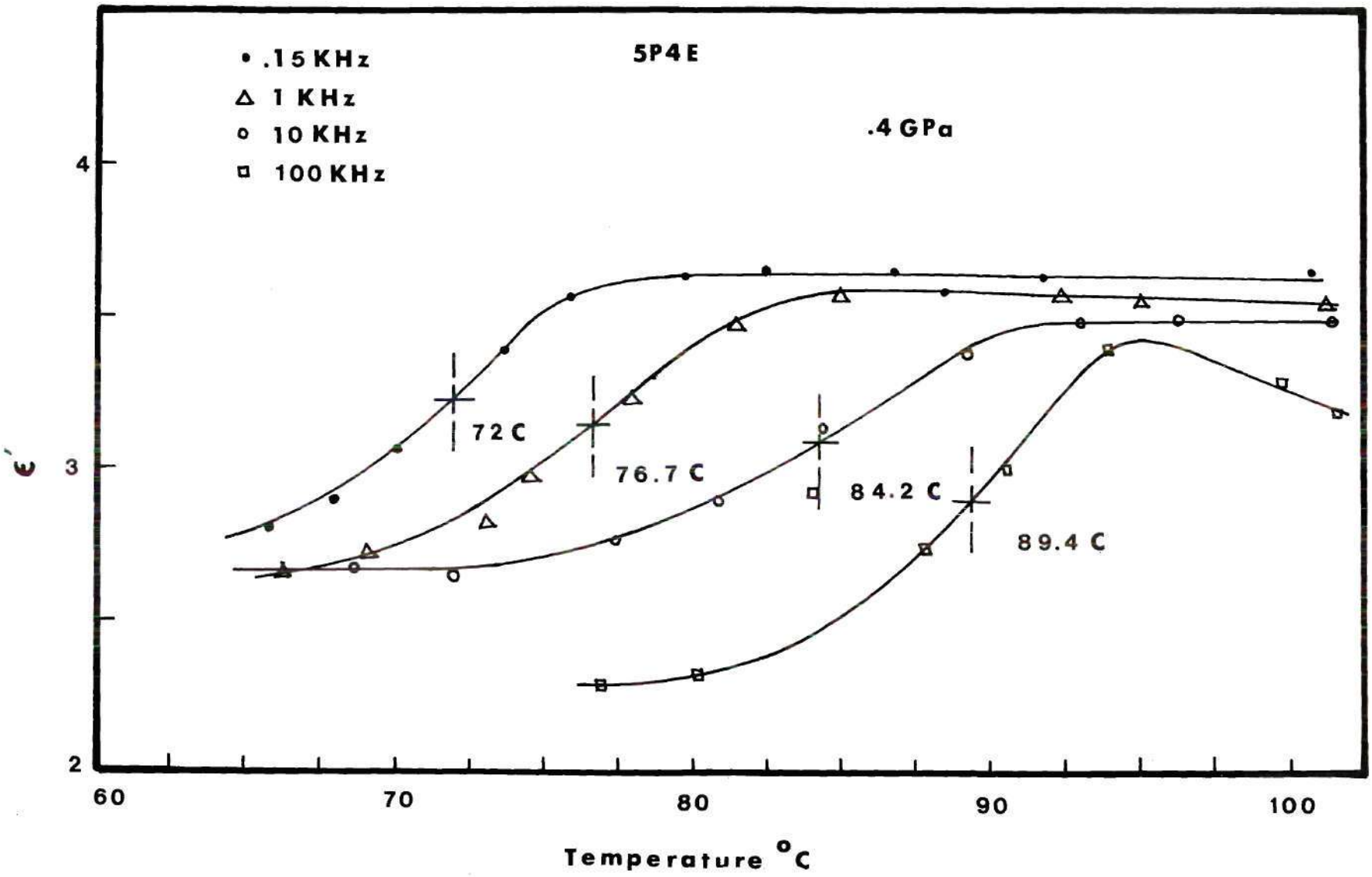

Figure 3. Permittivity of 5P4E at 414 MPa [56].

temperature of poly (vinyl acetate) has been studied over a wide range of rates by Kovacs [15]. The volume-temperature response obtained from different constant rates of cooling of a glass-forming substance is shown in Figure 4. Since decreasing the rate of cooling increases the effective experimental time. The viscoelastic transition temperature will be shifted to lower values. Matsouka and Maxwell [16] studied the effect of rate of compression. On the compressibility curves of polystyrene at 121 C, their results indicate that viscoelastic transition pressure, P_V, shifts to lower values when a greater rate of pressure application is employed. If the pressure is increased slowly, the molecules of the material will have enough time to rearrange and the viscoelastic transition will take place at a higher pressure. On the other hand, if the rate of pressurization is increased, the time for any structural changes is smaller and the viscoelastic transition occurs at a lower pressure.

The influence of thermodynamic history on viscoelastic transition of poly (vinyl acetate) was studied by McKinney and Goldstein [17] by using three different thermodynamic histories: variable formation history (isobaric cooling at different pressures), and two constant formation histories (cooling at atmospheric pressure or 80 MPa (800 bar) followed by pressure changes in the glassy state).

D. Techniques for the Determination of Viscoelastic Transition Temperature

Several techniques are employed for the determination of viscoelastic transition temperature, such as dilatometry [10,17,18], differential scanning calorimetry [19,20,21], thermomechanical analysis (TMA),

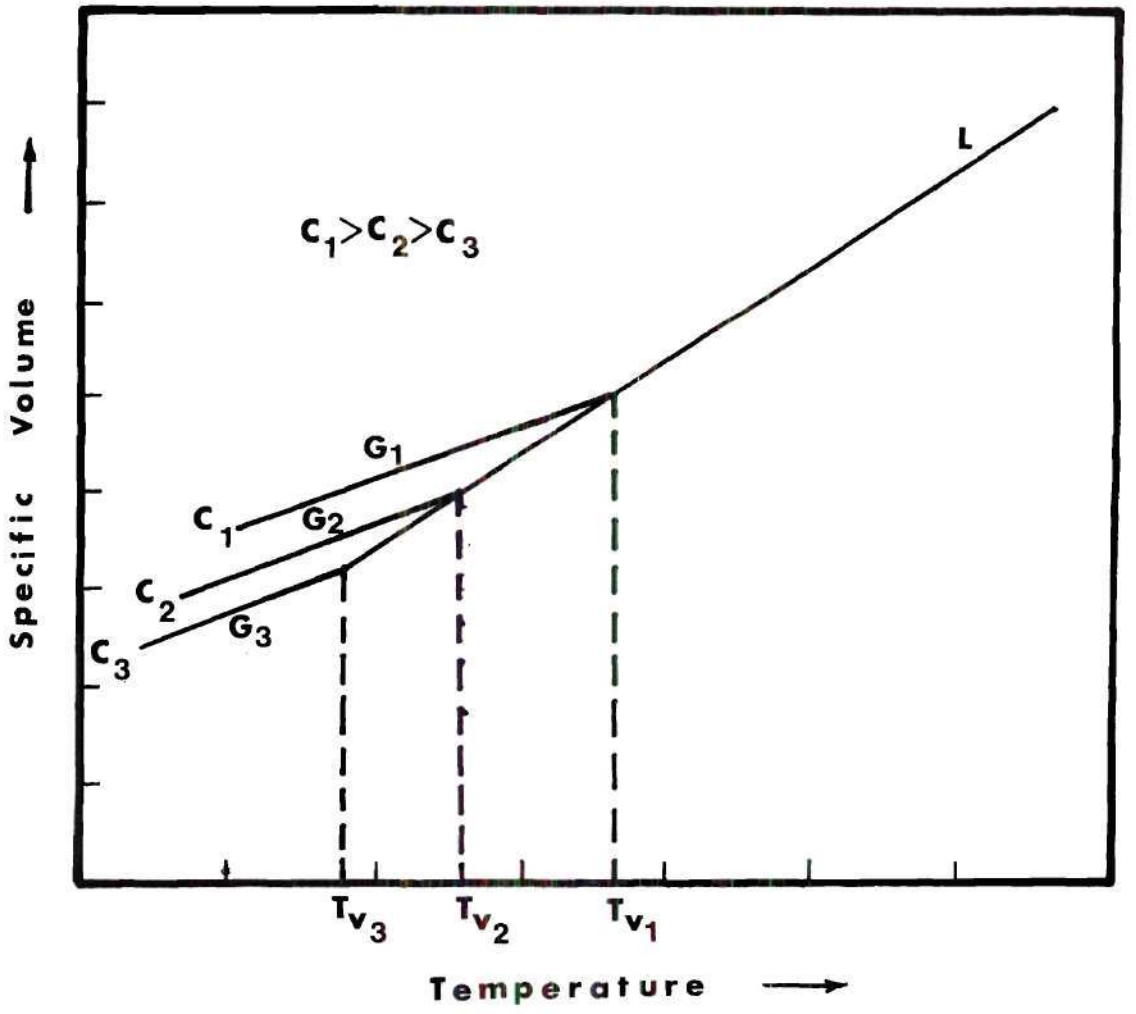

Figure 4. Dependence of the Viscoelastic Transition Temperature on the Cooling Rate, C_i. L = Liquid and G = Glass [8].

dielectric [22,23], light-scattering [8,24-34] and dynamic mechanical techniques [11,13,14,42-54]. Depending on the technique used, various methods exist for specifying the viscoelastic transition temperature within the transition region. The usual diatometric technique is to cool the liquid at a constant rate and extrapolate the linear portions of the volume-temperature relation above and below the transition region to their intersection. The temperature of this intersection [17] is taken as the viscoelastic transition temperature as shown in Figure 2. If T_V is measured by the change in the expansion coefficient or the specific heat, then T_V is taken as the mid-point in the step-change as measured from the extensions of the glass and liquid base lines as shown in Figure 1.

In the light scattering technique, a laser beam is used and the velocity of sound in materials is measured as a function of pressure and temperature [8]. The change in slope of the sound velocity as a function of pressure or temperature allows the determination of viscoelastic transition temperature as shown in Figure 5.

In the dielectric technique [11,14,55], the fluid is subjected to an alternating electric field. The permittivity ϵ' and the loss tangent, ϵ'' of the fluid are measured as a function of frequency, temperature and pressure. The temperature at which the loss tangent is maximum at a given frequency is recorded as the transition temperature for that frequency and pressure as shown in Figure 6. This transition temperature corresponds well with the midpoint temperature of the change in permittivity in most cases as shown in Figure 3 [56].

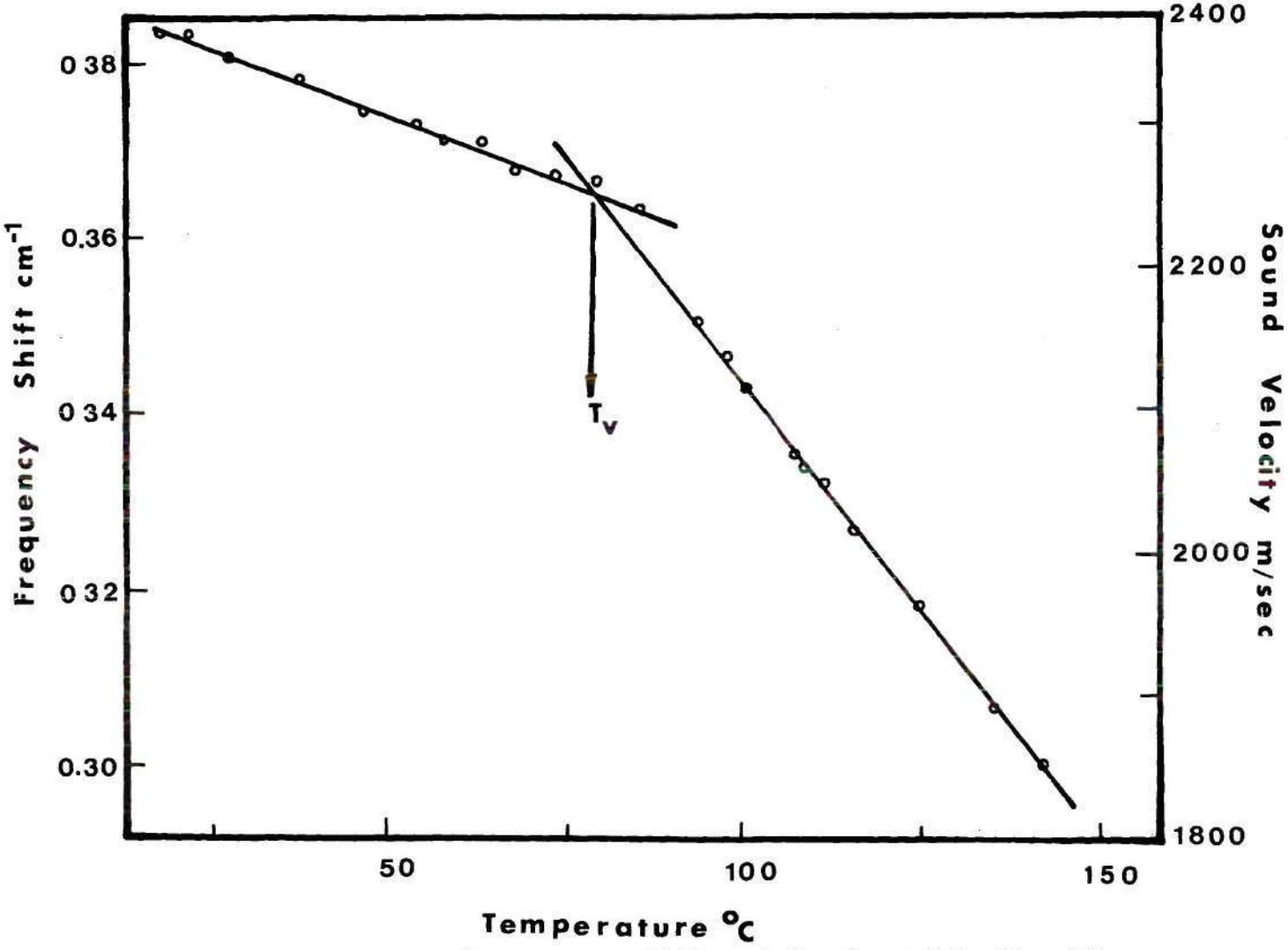

Figure 5. Variation of the Brillouin Frequency Shift and the Sound Velocity with Temperature at Atmospheric Pressure for Atactic Polystyrene [8].

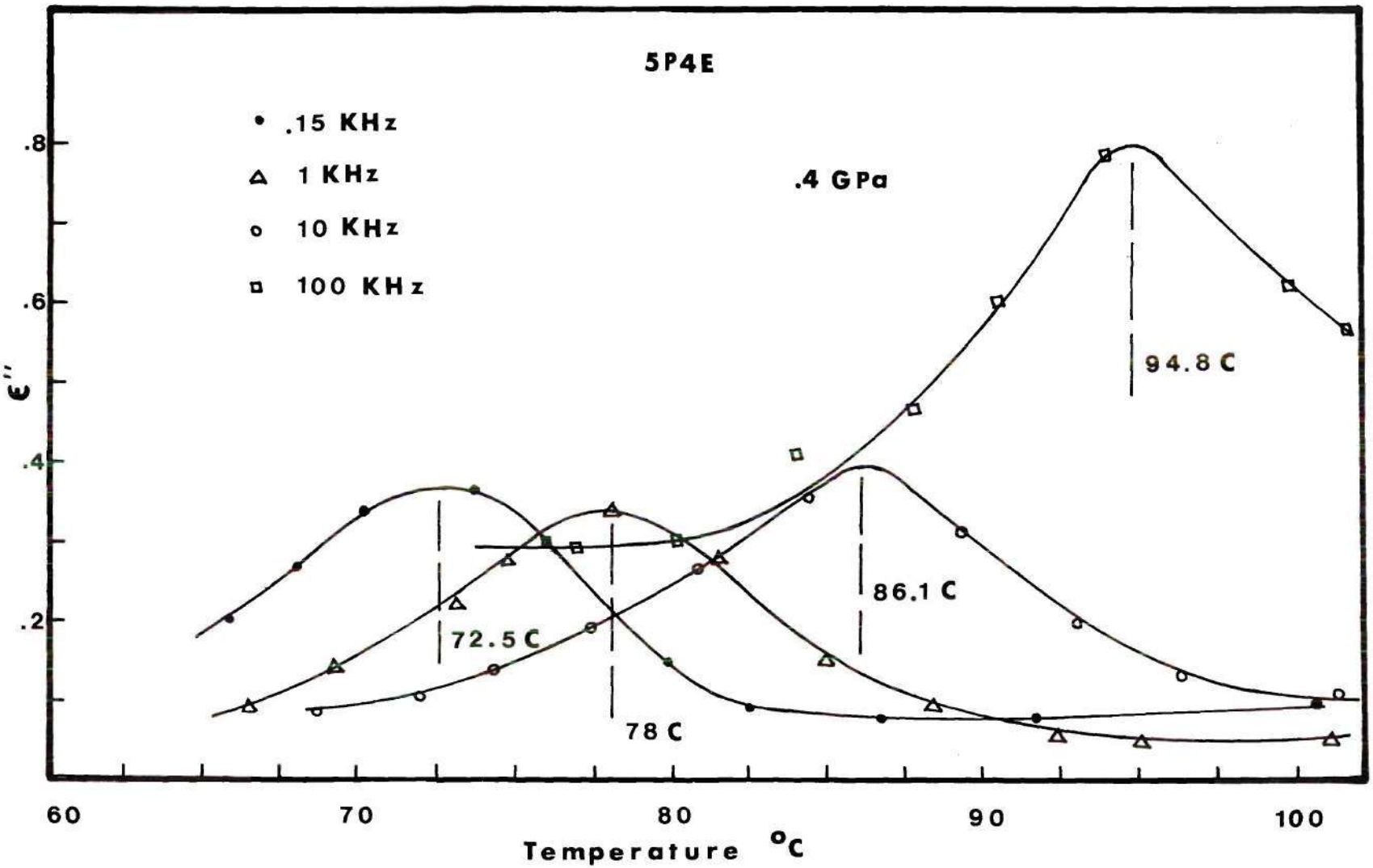

Figure 6. Dielectric Loss Tangent of 5P4E at 414 MPa [56].

In the dynamic mechanical technique a sinusoidally varying mechanical shear force is applied to the fluid. The strain produced in the fluid and the phase difference between the applied stress and resulting strain are measured. From these data, the real and imaginary parts of the shear modulus (G',G") can be determined. The plot of G' and G" as a function of temperature, frequency and pressure allows the determination of viscoelastic transition temperature. This technique is discussed in detail in Chapter II.

While the choice is somewhat arbitrary, and other authors have suggested alternate techniques, the above methods are the most commonly used. Because of these different ways of defining T_V for different experiments, and because of the different inherent cooling rates and histories in the different experiments, different viscoelastic transition temperatures may be measured on the same material in different experiments.

E. Need for Present Research

The mechanical behavior of a lubricant as it passes through an EHD contact, has been assumed by many workers to be viscous in nature [8]. The proposition that this behavior might not be that of a viscous liquid but an elastic solid was first presented by Smith [37] in 1960. In 1973 Johnson and Roberts [38] devised a rolling contact experiment to make direct observations of viscoelastic behaviors under conditions of elastohydrodynamic lubrication. Their results demonstrate a transition from a predominantly viscous to predominantly elastic response with increasing pressure at constant temperature and with decreasing

temperature at constant pressure. Johnson and Cameron [39] also showed a remarkable change in physical properties of the oil (Shell Turbo 33) at high pressure. In a recent paper [40] on a five ring polyphenyl ether, it was concluded that this oil behaves elastically and that the criterion of elastic behavior is not the magnitude of the pressure but of apparent viscosity.

It is important to note that most hydrocarbon lubricating oils contain linear and highly branched hydrocarbons as well as ring structures. Thus, a lubricant can display both a viscoelastic transition temperature which is associated with the non-crystallized part of the oil and a phase transition which is associated with the wax in the oil [19,41]. Viscoelastic transition temperatures at atmospheric pressure are -59 C for N1 sample and -21 C for 5P4E. Since these values are low compared to the operating temperatures in a typical EHD contact, the occurrence of the viscoelastic transition phenomena in the contact were not investigated earlier. However, because of the fact that the viscoelastic transition temperature increase with pressure, and because of the existence of high pressures in the EHD contacts, the viscoelastic transition temperature can be greater than the operating temperature in contact. For typical lubricants, the viscoelastic transition temperature increases with pressure at a rate ranging from 0.08 to 0.32 C per MPa. Thus, it would be expected that lubricants will be in the glassy state in an EHD contact with average pressures of 0.7 GPa or higher at room temperature. Therefore, it would be expected that many lubricants are in the glassy state for a significant portion of time they are in contact. Since the relaxation time of a material in the glassy state

is long compared to the residence time in the contact, it is possible that once in the glassy state, the lubricant will remain in the glassy state on the moving surface while the surface moves from one EHD contact to the next. Therefore, viscoelastic transition temperature as a function of pressure and frequency, is a significant material property of lubricants.

Shear mechanical relaxation is more relevant than other methods of determination of viscoelastic transition temperature, as far as its application to elastohydrodynamic lubrication is concerned. Having dielectric relaxation data at and above atmospheric pressures, the shear mechanical relaxation data at atmospheric pressure can be extrapolated to pressures above atmospheric pressure. Therefore, the determination of viscoelastic transition temperature of lubricants subjected to mechanical shear is very important for EHD.

CHAPTER II

RESEARCH TECHNIQUE

A. Theory of Viscoelastic Transition in Dynamic Measurement

For a perfect elastic material any imposed stress is proportional to the resulting strain (assumed small). If the imposed stress is removed, the strain is completely recovered. In addition, the work done during the application of stress is stored as strain energy which is completely recovered after the stress is removed. For a Newtonian fluid the imposed stress is proportional to the rate of strain (velocity). When the stress is removed the deformation is irrecoverable, and the work done by the stress during deformation is completely dissipated in the evolution of heat in the material. A linear viscoelastic material displays combined elastic and fluid material properties. As a result, if a uniaxial stress is suddenly imposed on a specimen of a linear viscoelastic material which is held for a certain duration of time and released thereon (Figure 7a), the strain distribution for such a load history is found to be as shown in Figure 7b. Figure 7b indicates that after the load is removed the strain does not recover immediately as in the case of perfect elastic material, but recovers partially after infinite time. The unrecovered portion of strain is the permanent deformation due to viscous flow.

Now, suppose a specimen of a linear viscoelastic material is subjected to a periodic stress represented by

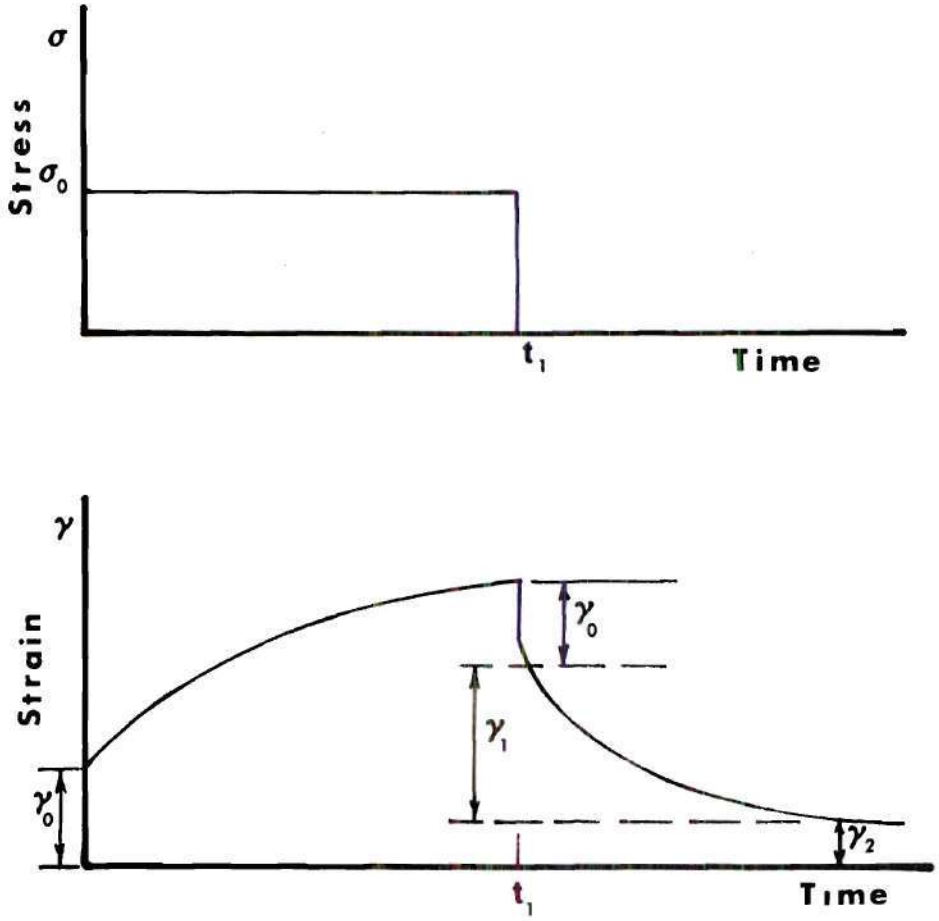

Figure 7. Stress and Strain Time Variation.

$$\sigma = \sigma_0 \, e^{i\omega t} \tag{1}$$

where σ_0 is stress amplitude, t is time, ω is circular frequency, and i is $\sqrt{-1}$. The strain is found to be also periodic but out of phase with stress as shown in Figure 8a. It is given by

$$\gamma = \gamma_0 \, e^{i(\omega t - \delta)} \tag{2}$$

where γ_0 is amplitude of strain and δ is phase angle between stress and strain. If the variation of stress and strain are both sinusoidal, a vector diagram involving these quantities can be drawn as shown in Figure 8b. The response of the material can be specified by a complex modulus representing the ratio of stress to strain. This is given by

$$G(i\omega) = \frac{\sigma}{\gamma} = \frac{\sigma_0}{\gamma_0} e^{i\delta} = \frac{\sigma_0}{\gamma_0} (\cos \delta + i \sin \delta) \tag{3}$$

where $G(i\omega)$ is the complex dynamic modulus corresponding to shear deformation. The complex modulus can be separated into a real part and imaginary part as

$$G(i\omega) = G'(\omega) + i\, G''(\omega) = \frac{\sigma_0}{\gamma_0} \cos \delta + i \frac{\sigma_0}{\gamma_0} \sin \delta \tag{4}$$

Therefore,

$$G' = \frac{\sigma_0}{\gamma_0} \cos \delta \tag{5}$$

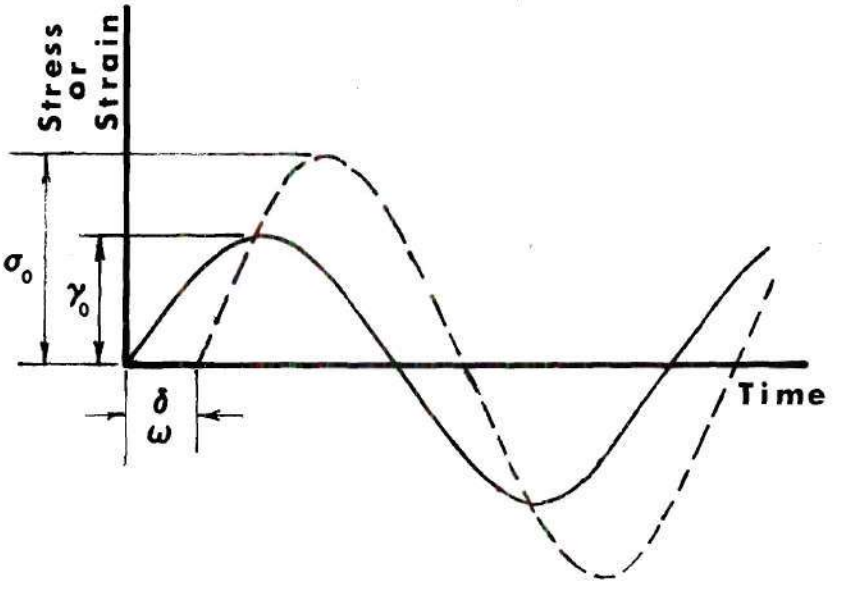

a. Sinusoidal Variation of Stress and Strain

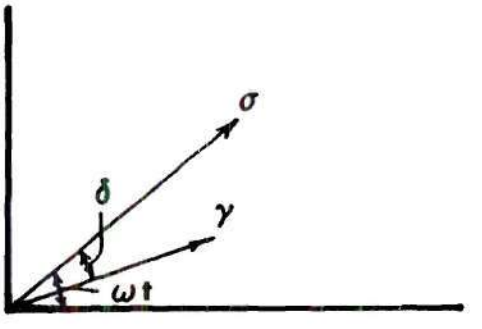

b. Vector Diagram for Sinusoidal Stress and Strain

Figure 8. Sinusoidal Stress and Strain

$$G'' = \frac{\sigma_0}{\gamma_0} \sin \delta \qquad (6)$$

Figures 8a and 8b indicate that the real part or the storage modulus represents the ratio of stress and strain in phase with the stress. Likewise, the imaginary part or the loss modulus represents the ratio of stress and the strain component, the latter being 90 degrees out of phase with the stress. The ratio of the loss modulus to the storage modulus is the tangent of the phase angle (usually called the loss tangent).

The nature of dynamic mechanical behavior of linear viscoelastic materials can be better understood by examining the variation of storage and loss modulus with frequency and temperature as shown in Figure 9. As indicated by the figure, the storage and loss moduli are both small at low frequencies or high temperature. The material is in liquid state in this region, displaying large deformation under loading. As the frequency is increased at constant temperature or the temperature is decreased at constant frequency, the storage modulus increases rapidly until it reaches a high constant value. The region where rapid increase in storage modulus takes place is usually referred to as the viscoelastic transition region. Therefore, the midpoint temperature of the change in storage modulus is the viscoelastic transition temperature of the material (See Figure 9). For many materials the transition region extends over at least six to ten decades of frequency. During the transition, the material displays considerable viscoelastic effect.

The loss modulus assumes a small value at low frequencies or high

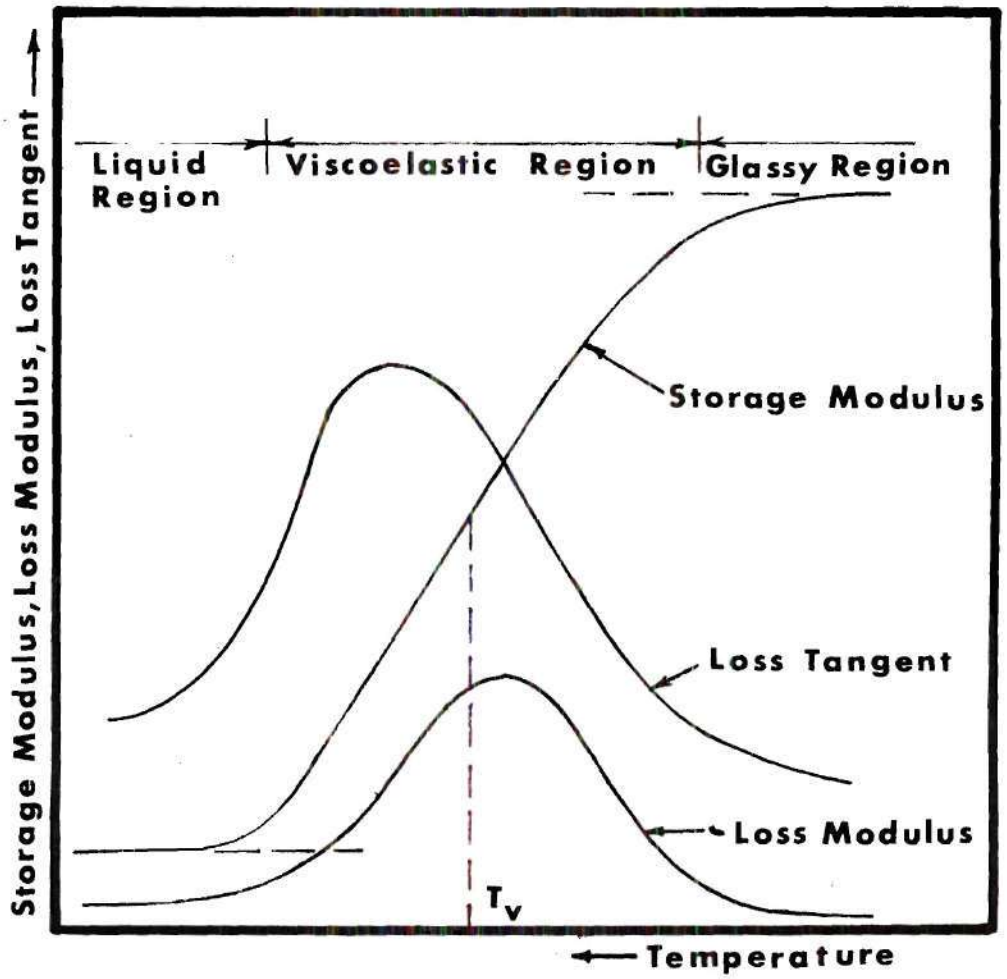

Figure 9. Variation of Storage Modulus Loss Modulus and Loss Tangent with Temperature

temperature. It first increases rapidly with decrease in temperature in the transition region until it reaches a maximum value. Thereafter it decreases rapidly and again assumes a small value at low temperature [Figure 9]. The temperature corresponding to the maximum value of loss modulus is the viscoelastic transition temperature and corresponds to the maximum energy loss in the material. Figure 9 also shows the variation of loss tangent with frequency and temperature. Just as in the case of loss modulus, the loss tangent reaches a maximum value in the transition region. However, the temperature at which this occurs is higher than the temperature at which the loss modulus becomes maximum.

B. Experimental Methods with Direct Measurement of Sinusoidally Varying Stress and Strain

The forces and displacements which are measured in a mechanical experiment are related to the states of stress and strain by the constitutive equation which describes the viscoelastic properties sought, as well as the equations of motion and continuity [13]. When inertial forces can be neglected and the deformations are infinitesimal, strain/stress ratios can be related to displacement/force ratios (or angular displacement/torque ratios) by form factors which depend on apparatus geometry. For most measurements on viscoelastic liquids, the deformation corresponds to simple shear: the most useful geometries are sketched in Figure 10, as follows: (a) parallel plate simple shear; (b) annular pumping; (c) rotation between coaxial cylinders; (d) torsion between cone and plate; (e) torsion of cylindrical disc between parallel plates; (f) axial motion between coaxial cylinders. All these geometries

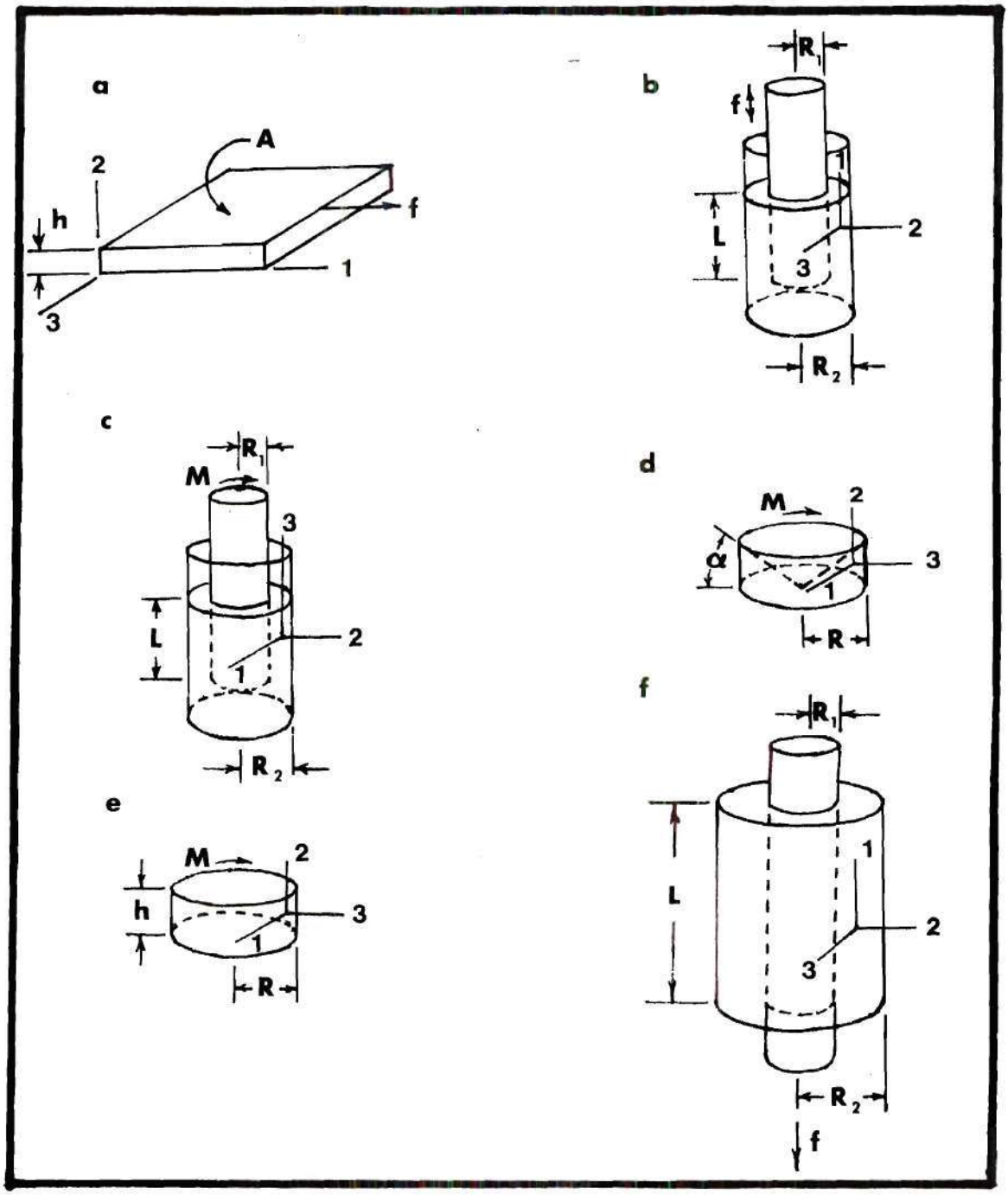

Figure 10. Geometries, Coordinates and Dimensions for Investigations of Viscoelastic Liquids [13].

give equivalent information for the shear strain/stress ratio, γ_{21}/σ_{21}, in small deformations. In the ratio γ_{21}/σ_{21}, both are periodic with a phase difference in oscillatory experiments. The geometrical factors [57] are expressed as follows:

(a) Parallel plate simple shear:

$$\gamma_{21}/\sigma_{21} = bx_1/f \tag{7}$$

$$b = A'/h \tag{8}$$

(b) Annular pumping:

$$\gamma_{21}/\sigma_{21} = bx_1/f \tag{9}$$

$$b = \frac{2\pi L}{(nq - (q^2 - 1)/(q^2 + 1)} \tag{10}$$

$$q = R_2/R_1 \tag{11}$$

(c) Rotation between coaxial cylinders:

$$\gamma_{21}/\sigma_{21} = b\alpha/M \tag{12}$$

$$b = 4\pi L/(1/R_1^2 - 1/R_2^2) \tag{13}$$

(d) Torsion between cone and plate:

$$\gamma_{21}/\sigma_{21} = b\alpha/M \tag{14}$$

$$b = 2\pi R^3/3\theta' \tag{15}$$

(e) Torsion between parallel plates:

$$\gamma_{21}/\sigma_{21} = b\alpha/M \tag{16}$$

$$b = \pi R^4/2h \tag{17}$$

(f) Axial motion between coaxial cylinders:

$$\gamma_{21}/\sigma_{21} = bx_1/f \tag{18}$$

$$b = 2\pi L/\ell n(R_2/R_1) \tag{19}$$

Here

b = form factor - dimensions cm in (a), (b) and (f); cm^3 in (c), (d) and (e)

x_1 = linear displacement

f = force

A' = area (of sample in contact with plates)

h = thickness of sample (See Figure 10)

L = length of sample (See Figure 10)

R_2 = radius of outer cylinder

R_1 = radius of inner cylinder

R = radius of sample (in cone and plate or parallel plate)

M = torque

α = angular displacement (radians)

θ' = angle between cone and plate

All these formulas are approximations in the sense that various edge and end effects have been neglected, as well as states of strain and flow

which may be somewhat more complicated than the simple forms assumed from the geometry. In some cases, better approximations have been introduced for specific experimental methods [13].

Now, for the coaxial cylinder geometry which has been used in this research, combination of equation (18) with equations (5) and (6) gives the components of the complex shear modulus:

$$G' = (f_0/bx_{01}) \cos \delta \tag{20}$$

$$G'' = (f_0/bx_{01}) \sin \delta \tag{21}$$

where f_0 and x_{01} are maximum (peak) values of force and displacement respectively, δ is the phase angle between force and displacement, and b is the form factor specified by equation (19).

If x_1 is sinusoidal, then

$$x_1 = x_{01} \sin \omega t \tag{22}$$

$$\dot{x}_1 = x_{01}\omega \cos \omega t = x_{01}\, \omega \sin \left(\omega t + \frac{\pi}{2}\right) \tag{23}$$

$$\ddot{x}_1 = -x_{01}\, \omega^2 \sin \omega t = x_{01}\, \omega^2 \sin(\omega t + \pi) \tag{24}$$

From equations (23) and (24) it is evident that velocity vector leads displacement vector by 90° and acceleration vector is 180° out of phase with displacement vector.

Elastic force (f_e) is directly proportional to displacement, therefore, it should be in phase with displacement, x_1. On the other hand, viscous force (f_V) is proportional to the rate of strain (velocity),

therefore it should be in phase with velocity and 90° out of phase with displacement. f_e and f_v are the two components of the force f, which is the response of a viscoelastic liquid to an imposed deformation in the absence of inertia. They are shown in Figure 14A.

So, evidently,

$$f_{0e} = f_0 \cos \delta \tag{25}$$

$$f_{0v} = f_0 \sin \delta \tag{26}$$

where f_{0e} and f_{0v} are peak values of elastic and viscous forces respectively.

Using equations (25) and (26) in equations (20) and (21) respectively, we obtain

$$G' = \frac{f_{0e}}{bx_{01}} \tag{27}$$

$$G'' = \frac{f_{0v}}{bx_{01}} \tag{28}$$

If displacement is sinusoidal, acceleration will also be sinusoidal as is evident from equation (24). If acceleration is represented by A_1, then

$$A_1 = A_{01} \sin(\omega t + \pi) \tag{29}$$

Comparing equations (24) and (29), we obtain

$$A_{01} = X_{01} \omega^2 \tag{30}$$

Using equation (30) in equations (27) and (28), we obtain

$$G' = \frac{\omega^2}{bA_{01}} f_{0e} \tag{31}$$

$$G'' = \frac{\omega^2}{bA_{01}} f_{0v} \tag{32}$$

C. Experimental Equipment

For this research coaxial cylinder geometry as shown in Figure 10f was selected. The schematic arrangement of the basic components of the shear mechanical relaxation experiment is shown in Figure 11.

The inner cylinder is in the form of a thin rod of spring steel of diameter 0.406 mm and length 35.6 mm. The outside cylinder is in the form of a thin shell of stainless steel of internal diameter 1.78 mm and length 5.1 mm. The rod is uniaxially silver soldered on a 10-32 NF screw so that it can be rigidly attached to the B & K impedance head type 8001 with the help of a nut and screw (See Figure 12). The shell is silver soldered to the hanger in such a way so as to make it coaxial with the rod when the set up is assembled (See Figure 12). The hanger is silver soldered to a base clamp which is rigidly clamped to the housing of the shaker. Therefore, slight adjustment in the center line of the shell can be done by inserting a packing between the clamp and the housing of the shaker.

The rod is sinusoidally oscillated by a B & K electromagnetic shaker type 4810 which operates longitudinally so as to cause the rod to move parallel to itself and the fixed shell. The electric power to

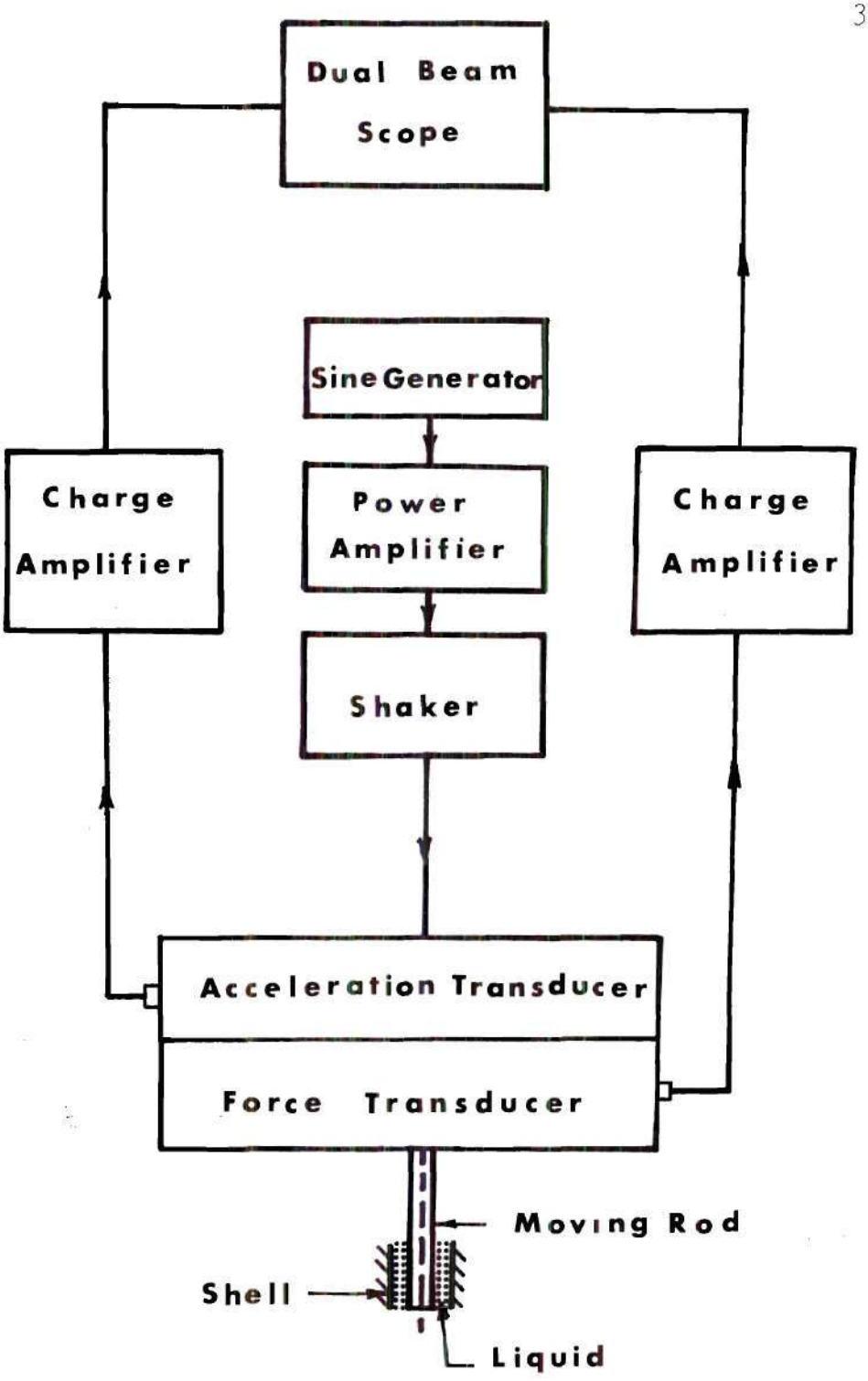

Figure 11. Schematic Arrangement of the Shear Mechanical Experiment

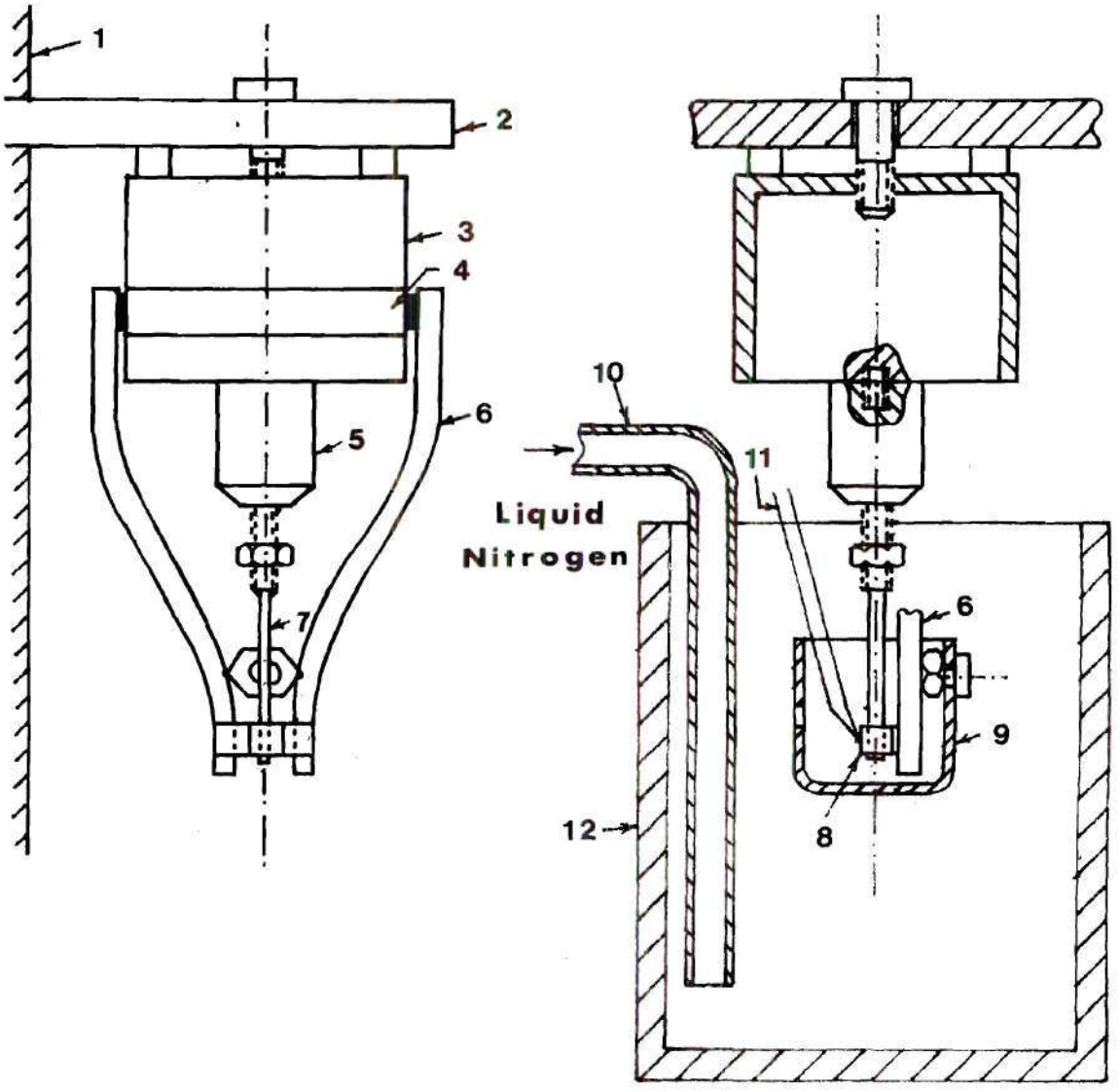

1. Wall, 2. Wooden Shelf, 3. Shaker, 4. Hose Clip,
5. Impedance Head, 6. Hanger, 7. Rod, 8. Shell, 9. Cup,
10. Copper Tube, 11. Thermocouple, 12. Dewar Flask

Figure 12. Schematic Diagram of the Experimental Set Up

the shaker is supplied by a B & K sine generator type 1042 through a Hewlett Packard power amplifier type 467A. The rod can be oscillated at any desired frequency in the range 5 - 10,000 Hz by setting the sine generator at that particular frequency. The amplitude of oscillation of the rod can also be varied by varying the voltage supply from the sine generator to the shaker.

The impedance head has two piezoelectric transducers - force and acceleration transducers (See Figure 11). The force transducer measures the force applied by the liquid sample in the gap on the rod and the acceleration transducer measures the acceleration of the liquid in direct contact with the rod.

The force and acceleration signals from the impedance head are fed to a dual beam oscilloscope through the Kistler charge amplifiers. Therefore, the peak values of force and acceleration, and the phase angle between them can be measured.

The shaker is rigidly attached to a big wooden shelf which, in turn, is rigidly attached to the wall (See Figure 12). This arrangement provides a very rigid mounting of the shaker and eliminates any vibration of the shaker itself which may cause error to the acceleration measurement of the liquid by the impedance head.

The rod is only very slightly projected outside the shell so as to minimize the effect of the liquid in the cup. The liquid in the cup is kept only at the top level of the shell and this is achieved by drilling a hole in the cup at that level (See Figure 12).

The sample liquid is cooled by the vapor of liquid nitrogen.

Liquid nitrogen is allowed to pass through a 920 mm long copper tube of 6.35 mm internal diameter so that by the time it reaches the dewar it is vaporized by gaining heat from the atmosphere (See Figure 12). The cup was made of copper and a few small holes were drilled in it so that nitrogen vapor passes through them thereby causing uniform and steady cooling of the liquid. Uniformity and rate of cooling have been observed by the author to be very important in this experiment.

Sensitivity of the force and acceleration transducers changes below 0 C. Therefore, air at room temperature is passed through the impedance head so as to keep its temperature high enough so that it's sensitivity is not appreciably effected.

Temperature of the liquid sample is measured by a copper-constantan thermocouple. One end of the thermocouple is silver soldered at the outside of the shell (See Figure 12) and the other end is immersed in a bath of ice and water, kept at 0 C. The voltage generated in the thermocouple is measured by a voltmeter. Temperature at the outside wall of the shell, then can be known by referring to the temperature-voltage chart for copper-constantan thermocouple. For more accurate measurement of T_V and for better comparison with dielectric measurement, temperature so measured was calibrated against temperature measured by a thermocouple inside the shell with liquid in it and the voltage generated in the thermocouple measured by a potentiometer (See Figure 13).

The formation of ice on the rod or in the gap between the rod and the shell adversely effect the result so special care was needed to avoid this situation by always keeping an atmosphere of nitrogen vapor around

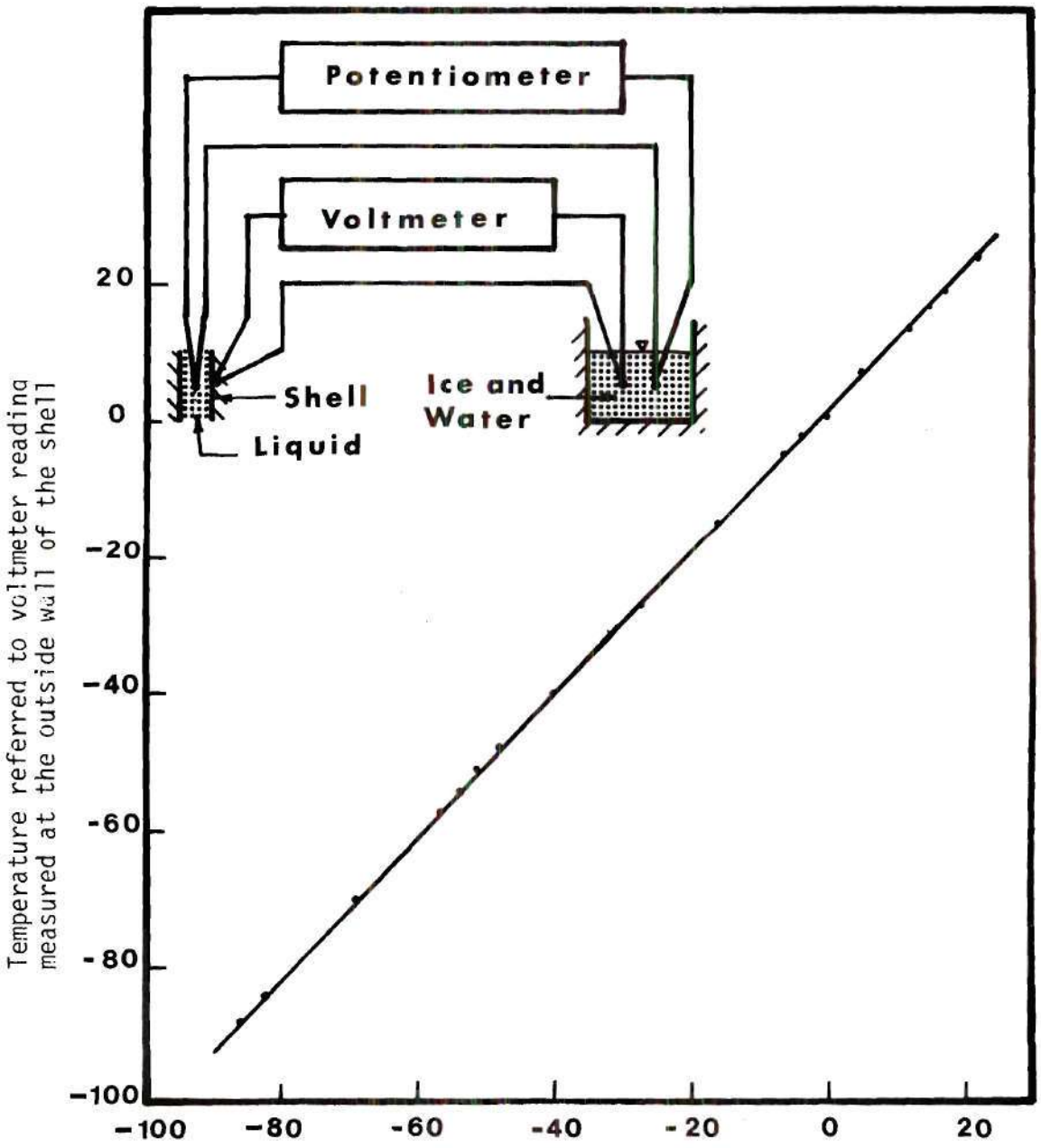

Figure 13. Temperature Calibration Curve

the rod. It was necessary to repeat the experiment if ice formed in this area.

D. Experimental Fluids

The seven lubricants investigated in this work are listed in Table 1 and a detailed description of each fluid is given in Appendix A. These lubricants were selected because of dielectric and dilatometric data on them available in our laboratory. In addition, these lubricants are representative of typical commercially available lubricants and research materials of current interest in the field of EHD lubrication [8].

Table 1. List of the Experimental Fluids

Symbol	Description
5P4E	Polyphenyl Ether
Santotrac 50	Synthetic Cycloaliphatic Hydrocarbon Traction Fluid
MCS 1218	Cycloaliphatic Hydrocarbon
Fyrquel 150 R&O	Tri-Aryl Phosphate
Krytox 143-AB	Perfluorinated Polymer
N1	Naphthenic Base Oil R-620-15
N2	N1 + 4% Poly Alkyl Methacrylate

CHAPTER III

EXPERIMENTAL PROCEDURE AND DATA REDUCTION

From equations (31) and (32), it is evident that if the acceleration of the liquid, and the elastic and viscous forces applied by the liquid can be measured. G' and G" can be determined.

The force transducer of the impedance head measures the total force (F) acting on its diaphragm. Therefore, it measures the sum of total force (f) applied by the liquid and the inertia force (f_i) of the rod (See Figure 11).

The force required to overcome the inertia of the rod is proportional to the rod acceleration and in phase with it. Therefore, this inertia force is 180^0 out of phase with elastic force as shown in Figure 14B. F is the vectorial summation of f_e, f_v and f_i (See Figure 14B). Here, θ is the angle between F and X_1.

Since we are interested in measuring the numerical value of G', we want to determine the numerical value of f_e which can be expressed at any instant of time as

$$f_e = F \cos \theta + f_i \tag{33}$$

Expressing equation (33) in terms of peak values, we obtain

$$f_{0e} = F_0 \cos \theta + f_{0i} \tag{34}$$

$$f_{0v} = F_0 \sin \theta \tag{35}$$

A

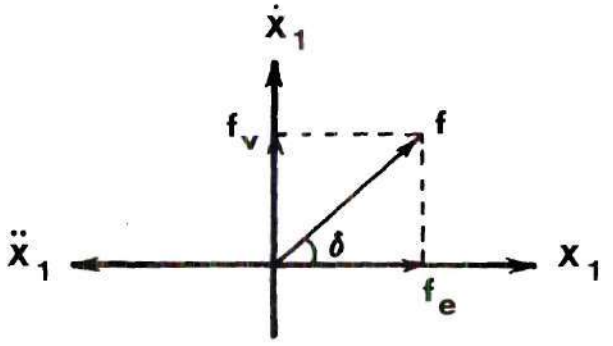

B

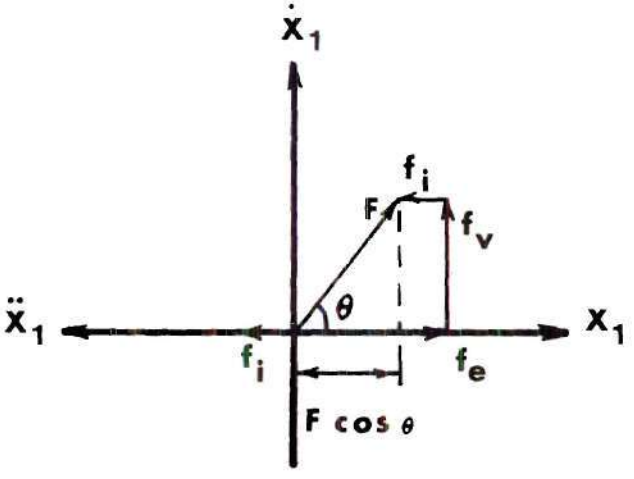

Figure 14. Vector Diagram for Elastic Force, Viscous Force and Inertia Force

The electrical characteristic of the impedance head rotates the acceleration vector by 180°, thereby bringing it in phase with displacement [62]. Therefore, the phase angle between force and acceleration as read on the oscilloscope, is equal to θ, the phase angle between F and X_1.

It is easier to measure the peak to peak value of the force and acceleration signals than to measure their amplitudes during experiment. If the peak to peak values are expressed by asterisks. Then equations (34), (35), (31) and (32) reduce to the following forms:

$$f^{*}_{Oe} = F^{*}_{O} \cos \theta + f^{*}_{Oi} \tag{36}$$

$$f^{*}_{Ov} = F^{*}_{O} \sin \theta \tag{37}$$

$$G' = \left(\frac{\omega^2}{bA'_{Ol}} \right) f^{*}_{Oe} \tag{38}$$

$$G'' = \left(\frac{\omega^2}{bA'_{Ol}} \right) f^{*}_{Ov} \tag{39}$$

Peak to peak values of force and acceleration can be measured from the following simple relations

$$f^{*}_{O} = E_f \times S_{Of} \times S_{Af} \tag{40}$$

$$A^{*}_{Ol} = E_A \times S_{OA} \times S_{AA} \tag{41}$$

where

f^{*}_{O} = peak to peak value of force in N

E_f = peak to peak value of force signal as read on oscilloscope in cm

S_{Of} = oscilloscope sensitivity in volt/cm

S_{Af} = charge amplifier sensitivity corresponding to the force transducer sensitivity set on it in N/Volt [63]

E_A = peak to peak value of acceleration signal as read on oscilloscope in cm

S_{OA} = oscilloscope sensitivity in Volt/cm

S_{AA} = change amplifier sensitivity corresponding to the acceleration transducer sensitivity set on it in g/volt

The peak acceleration of the rod is kept constant. Therefore, the inertia force of the rod remains constant during the experiment. The inertia force is measured at the particular frequency of interest at the beginning of the experiment before filling the liquid in the gap. As the liquid is cooled below room temperature, the value of F_0^* gradually increases. Therefore, the oscilloscope sensitivity needs to be decreased. Oscilloscope sensitivity for the acceleration signal is kept the same throughout an experiment. Charge amplifier sensitivities (S_{Af} and S_{AA}) are kept constant for the entire work.

Therefore,

$$F_0^* = E_F \times S_{OF} \times S_{Af} \tag{42}$$

$$f_{Oi}^* = E_{fi} \times S_{Of} \times S_{Af} \tag{43}$$

$$f_{Ov}^* = E_{fv} \times S_{Of} \times S_{Af} \tag{44}$$

$$A^{*}_{01} = E_A \times S_{OA} \times S_{AA} \tag{45}$$

Now, substituting equations (42), (43), (44) and (45) in equations (38) and (39), we obtain

$$G' = \left(\frac{S_{Af}}{S_{AA} \times b}\right)\left(\frac{E_F \cos\theta \cdot S_{OF} + E_{fi} \cdot S_{Of_i}}{E_A \, S_{OA}}\right)\omega^2 \tag{46}$$

$$G'' = \left(\frac{S_{Af}}{S_{AA} \times b}\right)\left(\frac{E_F \sin\theta \, S_{OF}}{E_A \, S_{OA}}\right)\omega^2 \tag{47}$$

The geometry factor (b) and the charge amplifier's sensitivity (S_{Af} and S_{AA}) were kept constant for the entire work. Therefore,

$$\frac{S_{Af}}{S_{AA} \times b} = \text{constant} = k \tag{48}$$

Using equation (48) in equations (46) and (47), we obtain,

$$\frac{G'}{K} = \left(\frac{E_F \cos\theta \, S_{OF} + E_{f_i} \, S_{Of_i}}{E_A \, S_{OA}}\right)\omega^2 \tag{49}$$

$$\frac{G''}{K} = \left(\frac{E_F \sin\theta \, S_{OF}}{E_A \, S_{OA}}\right)\omega^2 \tag{50}$$

As all quantities on the right hand side of equations (49) and (50) are known, the proportional values of G' and G" can be calculated at any temperature and frequency.

As discussed previously, the viscoelastic transition temperature is defined as the midpoint temperature of the change in G' with

temperature. The value of (G'/K), for all the liquids studied, was found to be very small at high temperature in the beginning of the experiment and was smaller in value by three or four orders of magnitude than that of the final value at low temperature after transition. So, viscoelastic transition temperature was considered as the temperature corresponding to half the maximum value of (G'/k). (G'/k) was plotted on the logarithmic scale due to the change of many orders of magnitude in its value. From the plot of log (G'/k) versus temperature, the viscoelastic transition temperature of the liquid at the frequency of the experiment can be found. The temperature of the liquid was measured at the outside wall of the shell. But a difference of about $1^{\circ}C$ was found between the temperature of the liquid inside the gap and that at the outside wall of the shell as is evident from the calibration curve (See Figure 13). Therefore, the viscoelastic transition temperature so obtained was corrected by referring to the calibration curve.

Knowing T_V at different frequencies, the transition curve of the liquid can be drawn by plotting log of frequency (ν) versus the reciprocal of T_V ($^{\circ}K$), as is the standard practice.

The experimental procedure is straightforward. Before taking any reading, the instruments are kept on for about 45 minutes which is required for the stabilization of the instruments. Then the sine generator is set at the frequency of interest and a particular value of the peak to peak acceleration of the rod without the liquid in the gap. The sensitivity of 2g per volt output of the charge amplifier and the oscilloscope sensitivity of .01 volt/cm, the peak to peak value

of the acceleration signal is 6 cm. At this value of acceleration, the peak to peak value of the force signal is recorded which is the value of the inertia force. Then liquid is introduced into the gap between the rod and the shell. The cup is also filled to the level of the overflow hole. The liquid is gradually cooled by the vapor of liquid nitrogen at an approximate rate of 0.25 - 0.5 C per minute. While keeping the acceleration constant, the peak to peak value of the force signal, the oscilloscope sensitivity for the force signal, the phase angle between the force and acceleration signals, and the temperature are recorded for every 2-3 C decrease in temperature. Data are taken until the change in the value of the force signal becomes small or negligible after which cooling is stopped. When the temperature of the liquid reaches the room temperature, the liquid in the cup is replaced and the experiment is repeated at different frequency. The change in sample was necessary to avoid the influence of condensed moisture in the sample after prolonged cooling.

CHAPTER IV

EXPERIMENTAL RESULTS

The figures presented in this chapter were obtained by the data reduction technique described in Chapter III. Log [G'/K] versus temperature curves are presented in Figures 15A-G. The viscoelastic transition temperatures (i.e., the temperature at which the storage modulus is one half its maximum value) and the temperature range employed for all the liquids are shown in Table 2.

For comparison purposes the mechanical shear transition curves are shown along with transition data from dielectric and dilatometric measurements* in Figures 16A-G. Finally, the mechanical shear viscoelastic transition behavior of the different liquids studied, are presented in Figure 17.

The effect of blending a polymer with the naphthenic base oil on the viscoelastic transition temperature is seen in Figure 17. The viscoelastic transition temperature for N2 occurred at approximately $0.7^{o}C$ higher than that of N1 at atmospheric pressure. This difference is comparable to the result of Alsaad [8]. The fact that the N2 transition temperature is than N1 is expected because the transition in polymers occurs at high temperatures than lubricating oils [8].

*These dielectric and dilatometric data were obtained in this laboratory by Mr. S. Bair under the same NASA grant. They will be published in a NASA contract report [56].

Viscoelastic transition temperature increases with frequency. It can be understood in terms of free volume which may be present as holes of the size of molecular dimensions or smaller voids associated with packing irregularities. Lowering of temperature is accompanied by collapse of free volume as the molecular adjustments take place [13]. At lower temperatures, the adjustments require more time to occur, and if crystallization does not occur a temperature is reached where the collapse can no longer occur on the time scale of the observation. Then the only residual contraction is of a solid-like character. This temperature is known as the viscoelastic transition temperature. At constant temperature, if frequency is increased, molecules vibrate more rapidly and therefore they need more free volume to rearrange themselves, so transition can be expected at higher temperature.

As the temperature is decreased, the free volume decreases. Therefore, the viscosity increases. On the basis of free volume, Arrhenius found the viscosity, η, to vary as an exponential function of the absolute temperature, T_o. The Arrhenius equation is expressed as

$$\ell n(\eta/A) = B/T \tag{51}$$

where A and B are constants.

From the Maxwell model, viscosity is found to be proportional to the relaxation time which is the reciprocal of the frequency ν at viscoelastic transition. Because viscosity varies with temperature according to equation (51), one would expect the transition curves to be logrithmic and therefore logically be plotted as Log ν versus 1/T.

Table 2. Viscoelastic Transition Temperature as Obtained by Mechanical Shear Measurements for Different Liquids at Atmospheric Pressure

Liquid	Range of Measurements °C	Frequency Hz	Viscoelastic Transition Temperature °C
5P4E	20 to -15	100	- 9.3
		300	- 5.5
		1000	- 4
Santotrac 50	20 to -80	100	-58
		500	-53.25
		1000	-50.8
N1	20 to -72.5	100	-59.75
		300	-57.25
		1000	-55.2
N2	20 to -67.5	100	-60
		300	-56
		1000	-53.5
Fyrquel 150	20-to-50	100	-41
		300	-38.5
		1000	-36.75
Krytox	20 to -65	100	-57
		300	-55
		1000	-53
MCS 1218	20 to -22.5	100	-16.5
		300	-13.25
		1000	-10

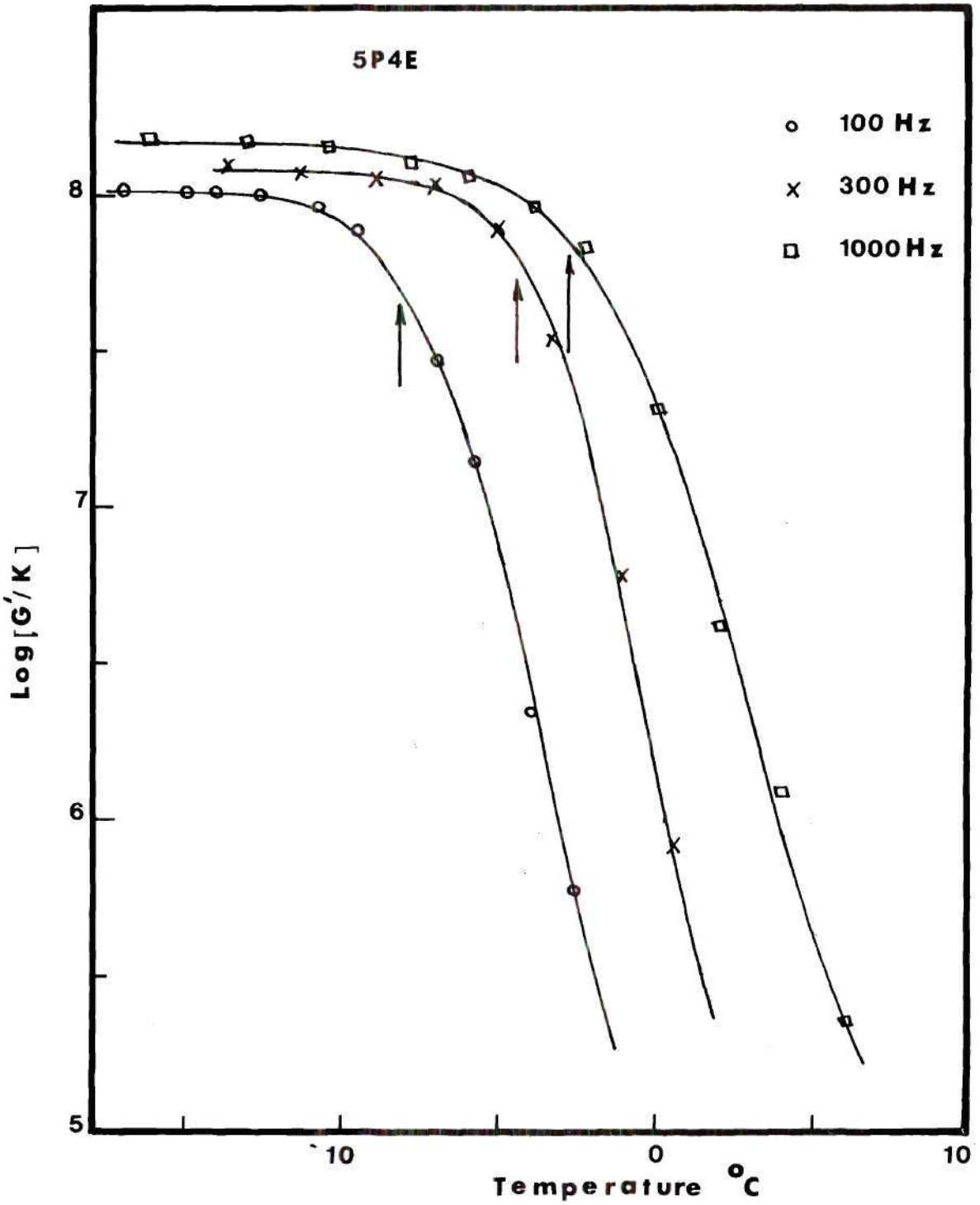

Figure 15-A. Variation of G'/K with Temperature for 5P4E at Atmospheric Pressure. Arrows indicate the Visco-elastic Transition Temperature

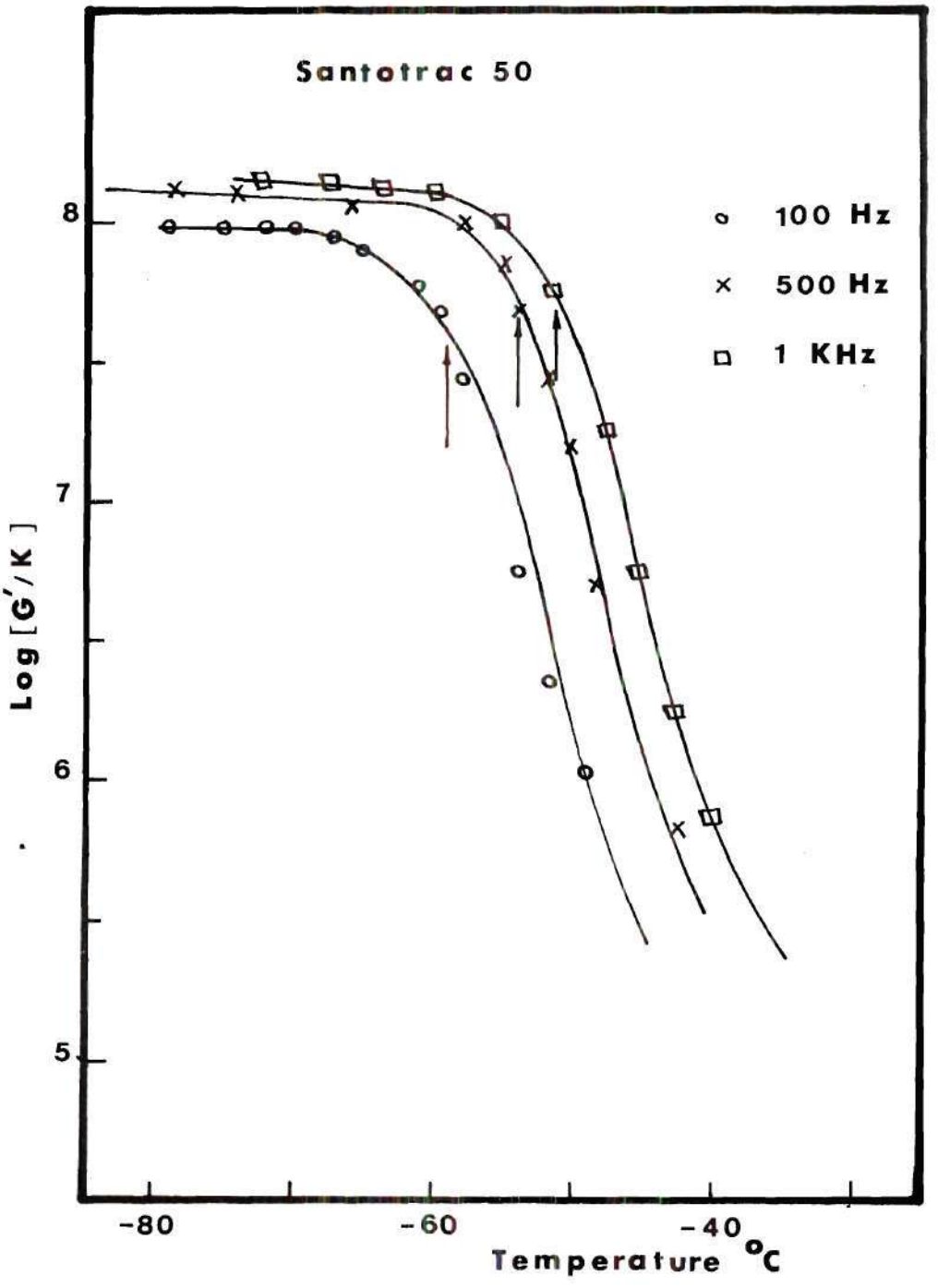

Figure 15-B. Variation of G'/K with Temperature for Santotrac 50 at Atmospheric Pressure. Arrows indicate the Viscoelastic Transition Temperature

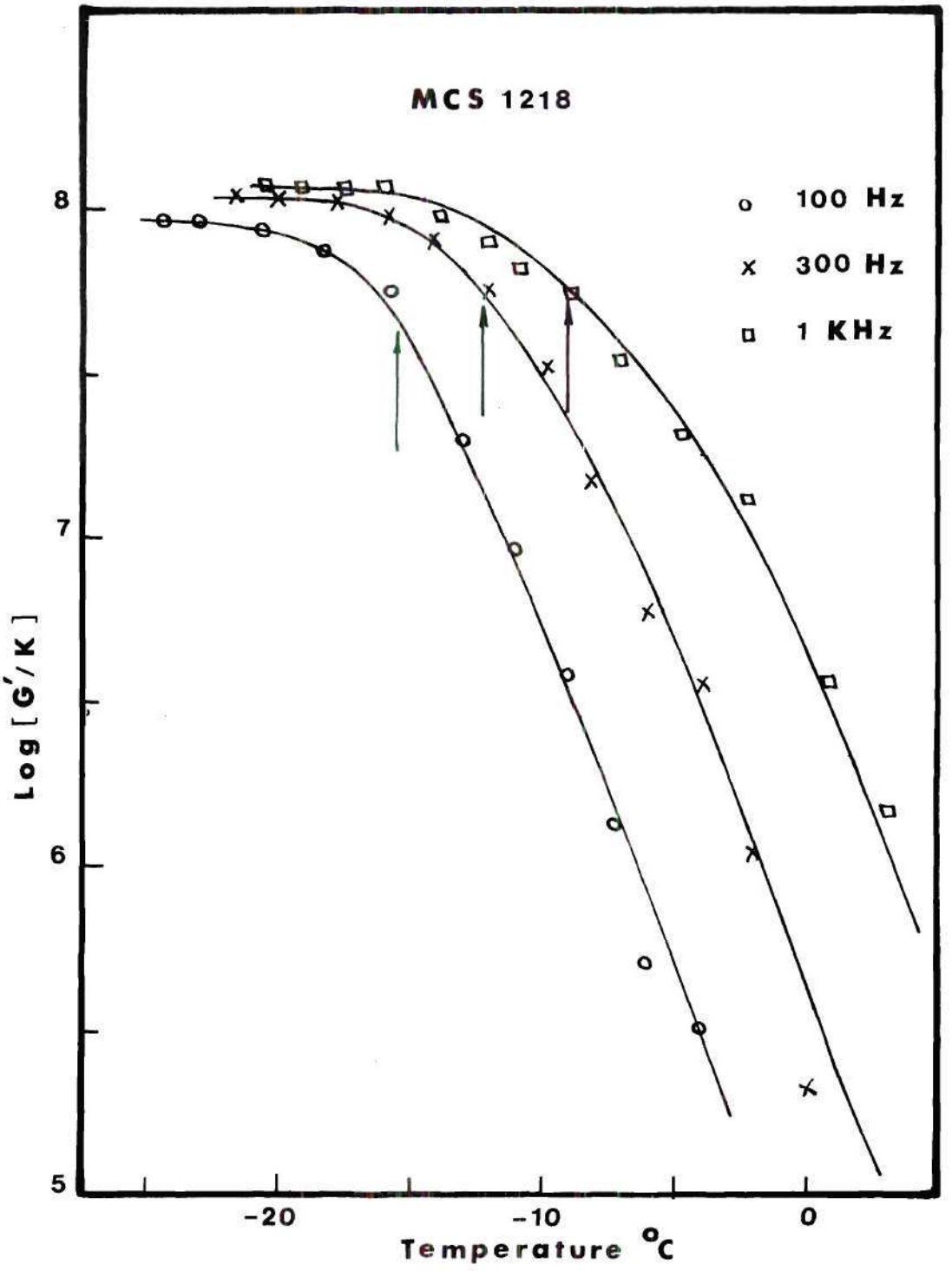

Figure 15-C. Variation of G'/K with Temperature for MCS 1218 at Atmospheric Pressure. Arrows indicate the Viscoelastic Transition Temperature

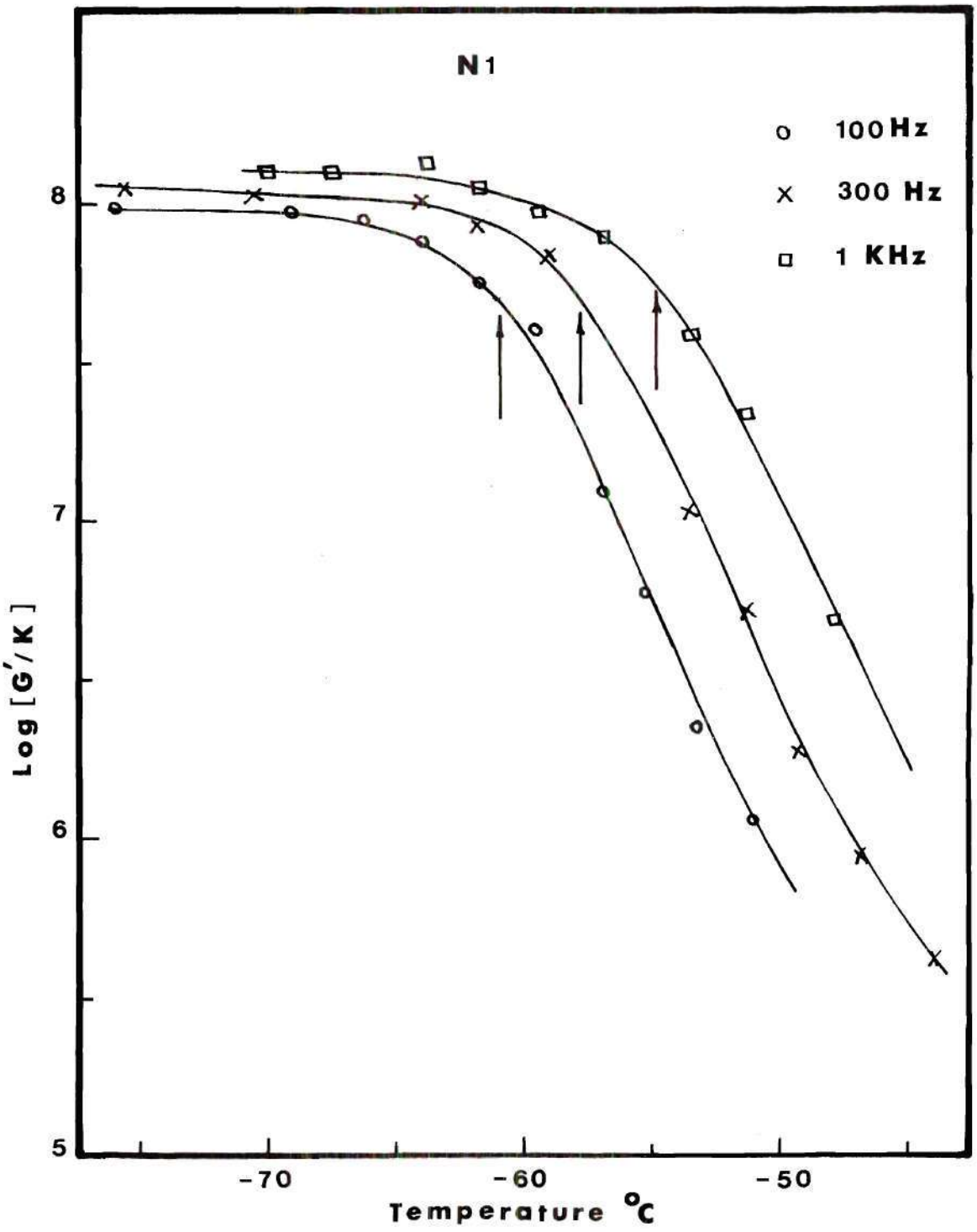

Figure 15-D. Variation of G'/K with Temperature for N1 at Atmospheric Pressure. Arrows indicate the Viscoelastic Transition Temperature

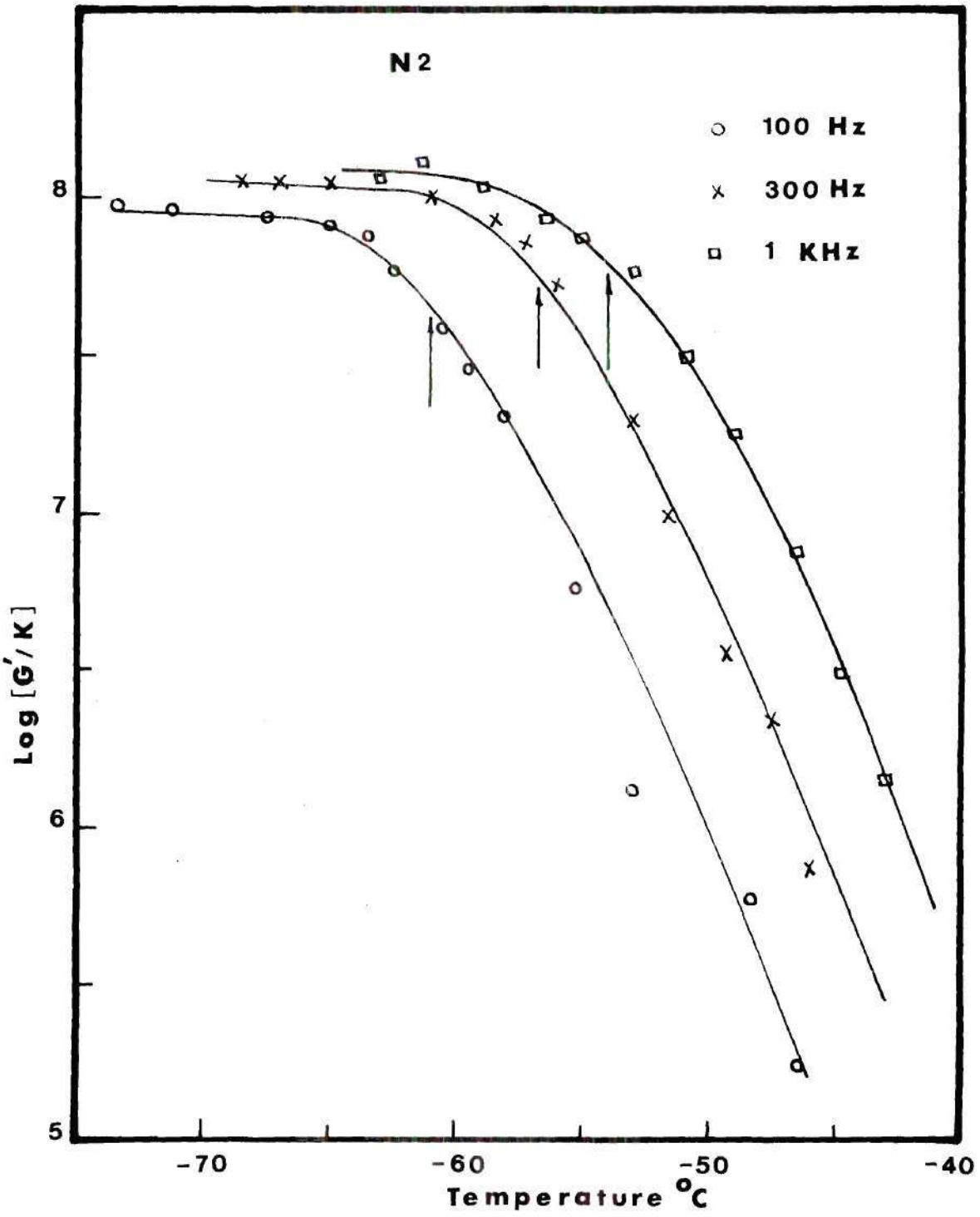

Figure 15-E. Variation of G'/K with Temperature for N2 at Atmospheric Pressure. Arrows indicate the Viscoelastic Transition Temperature

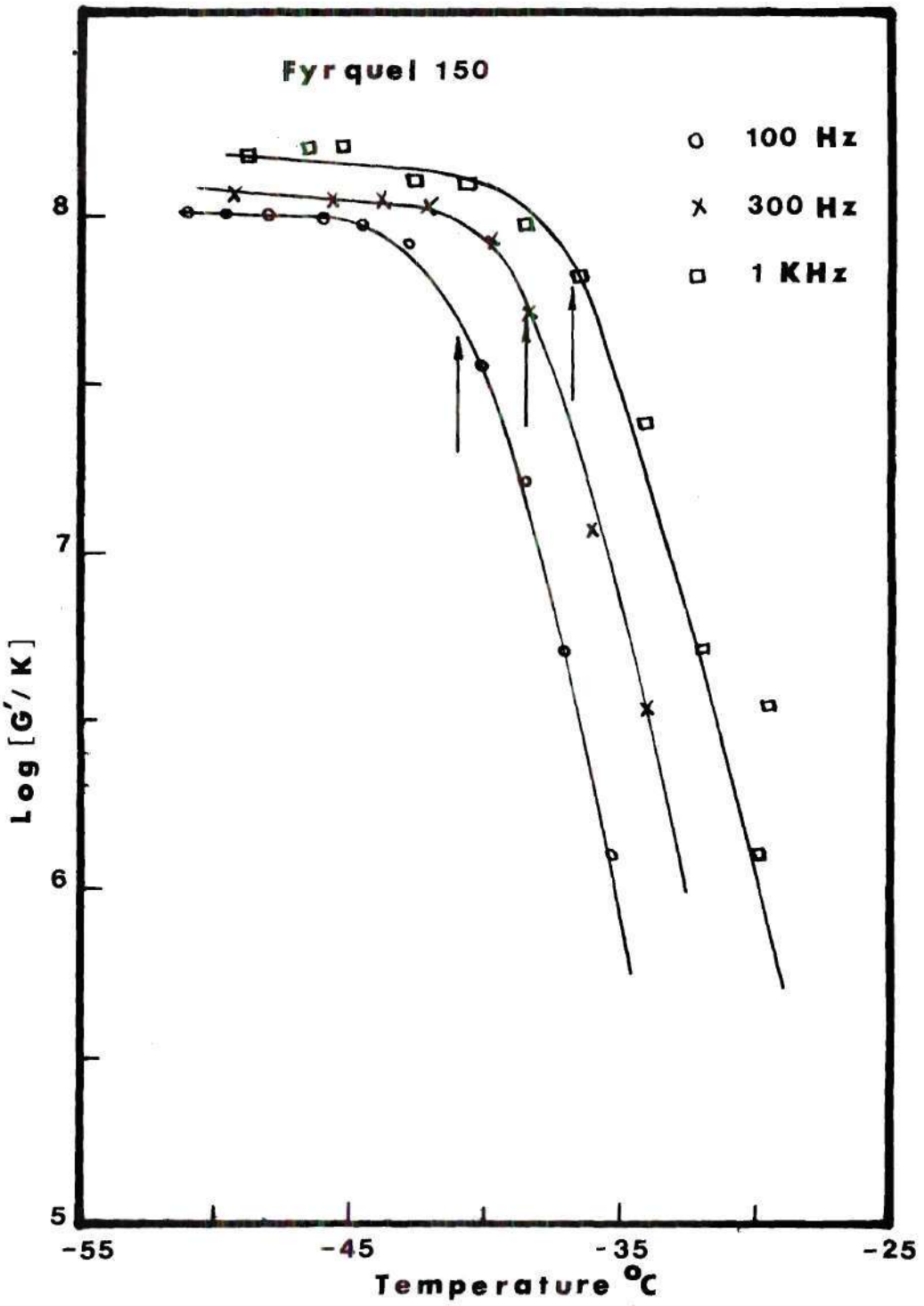

Figure 15-F. Variation of G'/K with Temperature for Fyrquel 150 at Atmospheric Pressure. Arrows indicate the Viscoelastic Transition Temperature

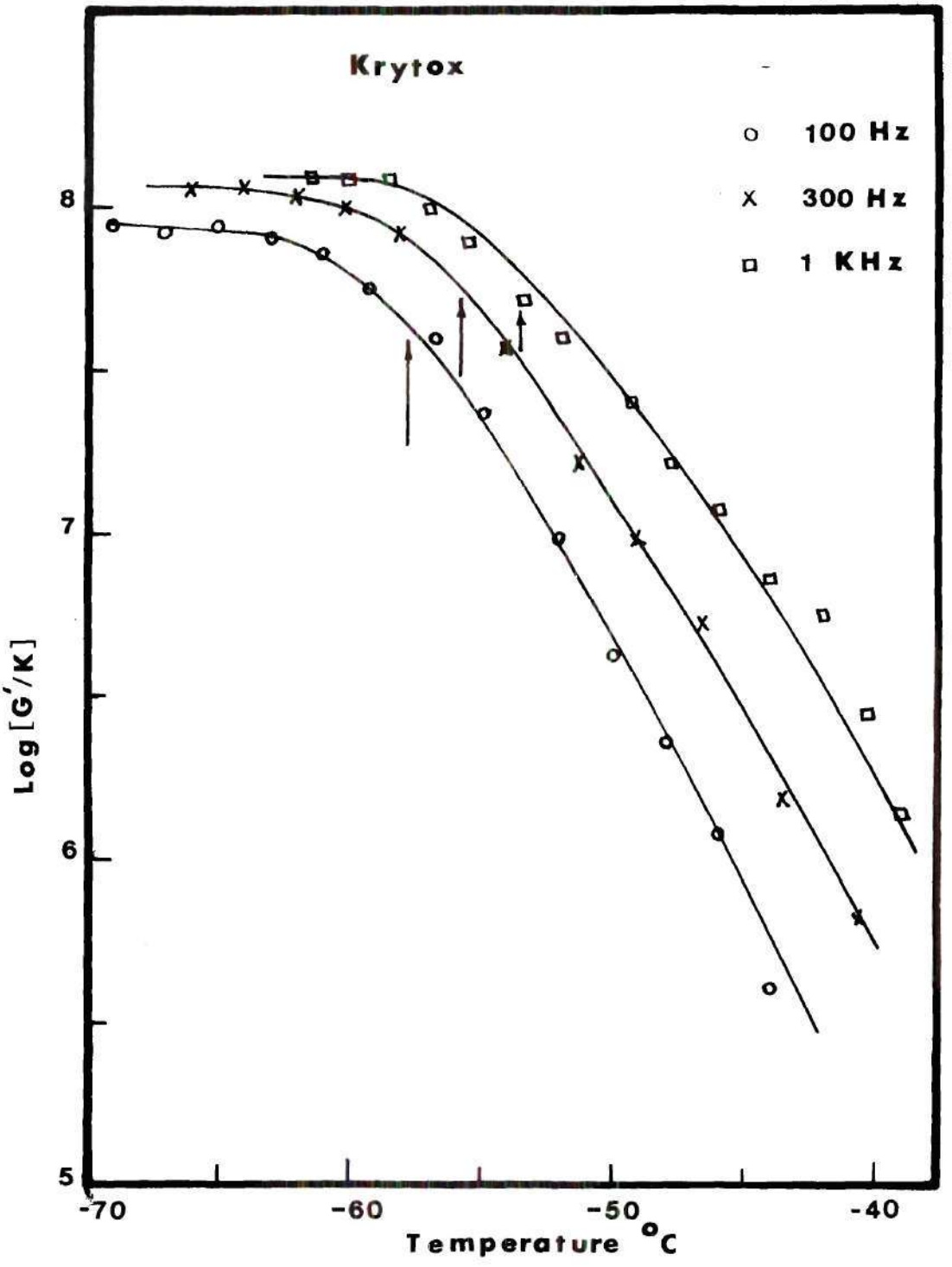

Figure 15-G. Variation of G'/K with Temperature for Krytox at Atmospheric Pressure. Arrows indicate the Viscoelastic Transition Temperature

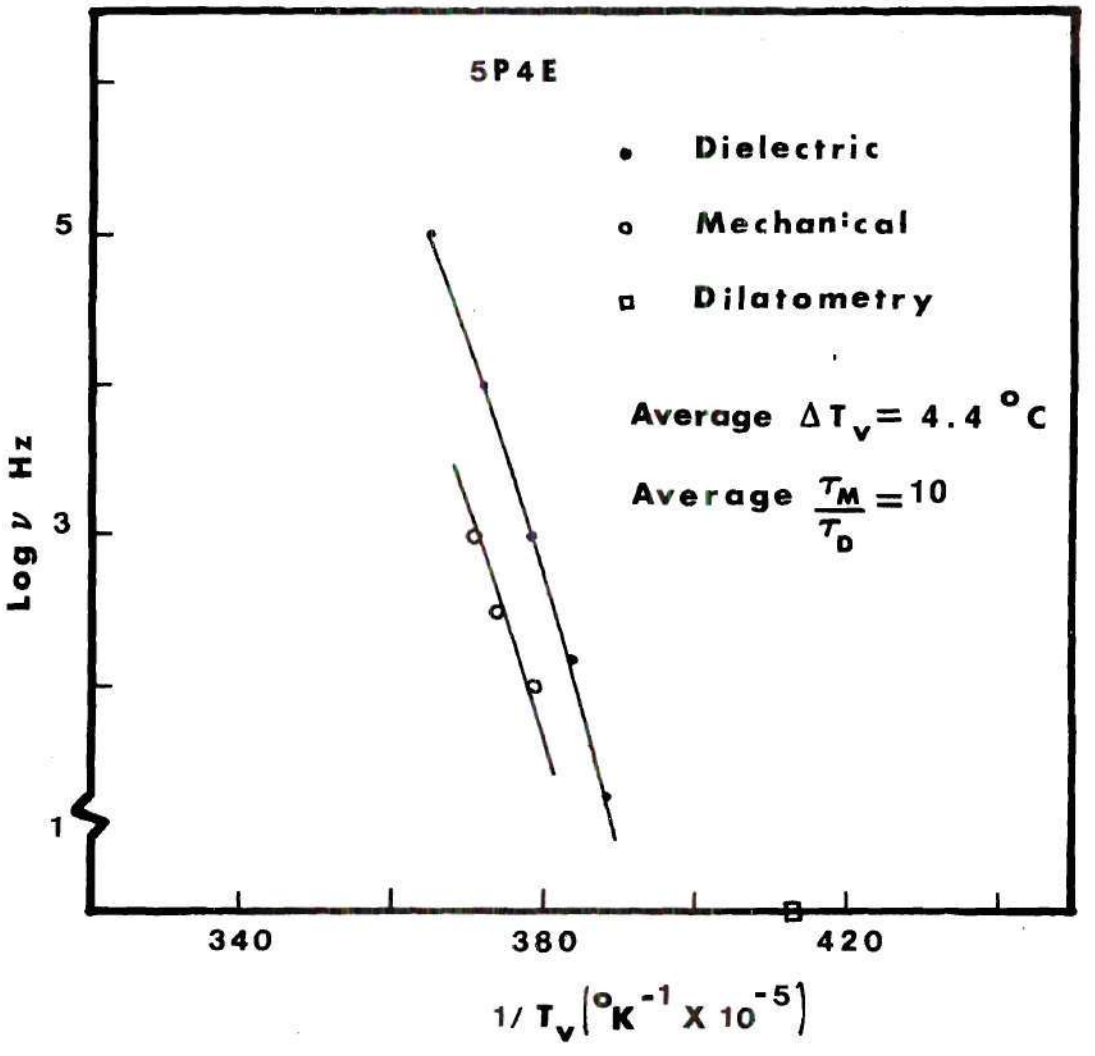

Figure 16-A. Viscoelastic Transition Curves for 5P4E at Atmospheric Pressure

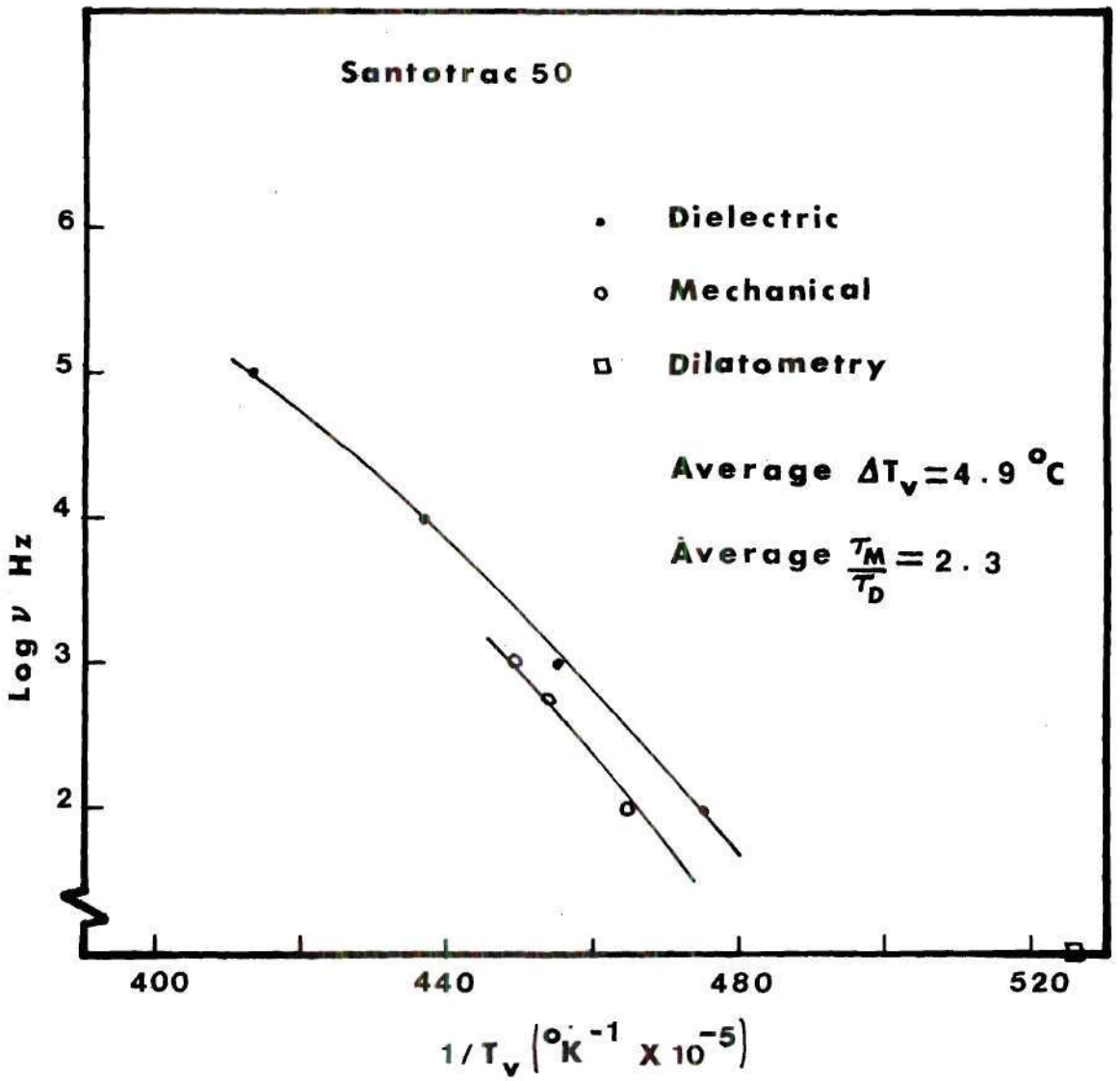

Figure 16-B. Viscoelastic Transition Curves for Santotrac 50 at Atmospheric Pressure

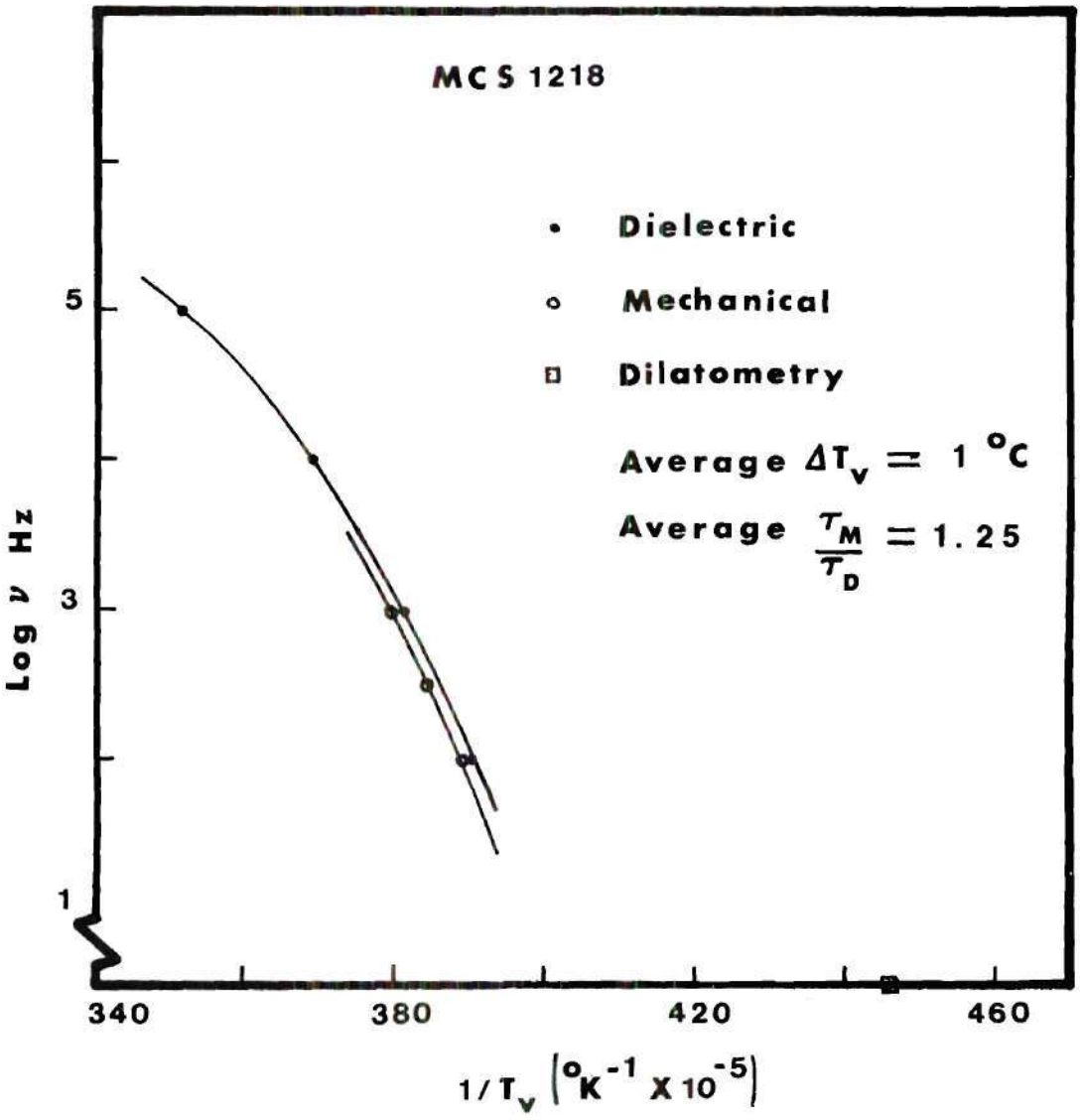

Figure 16-C. Viscoelastic Transition Curves for MCS 1218 at Atmospheric Pressure

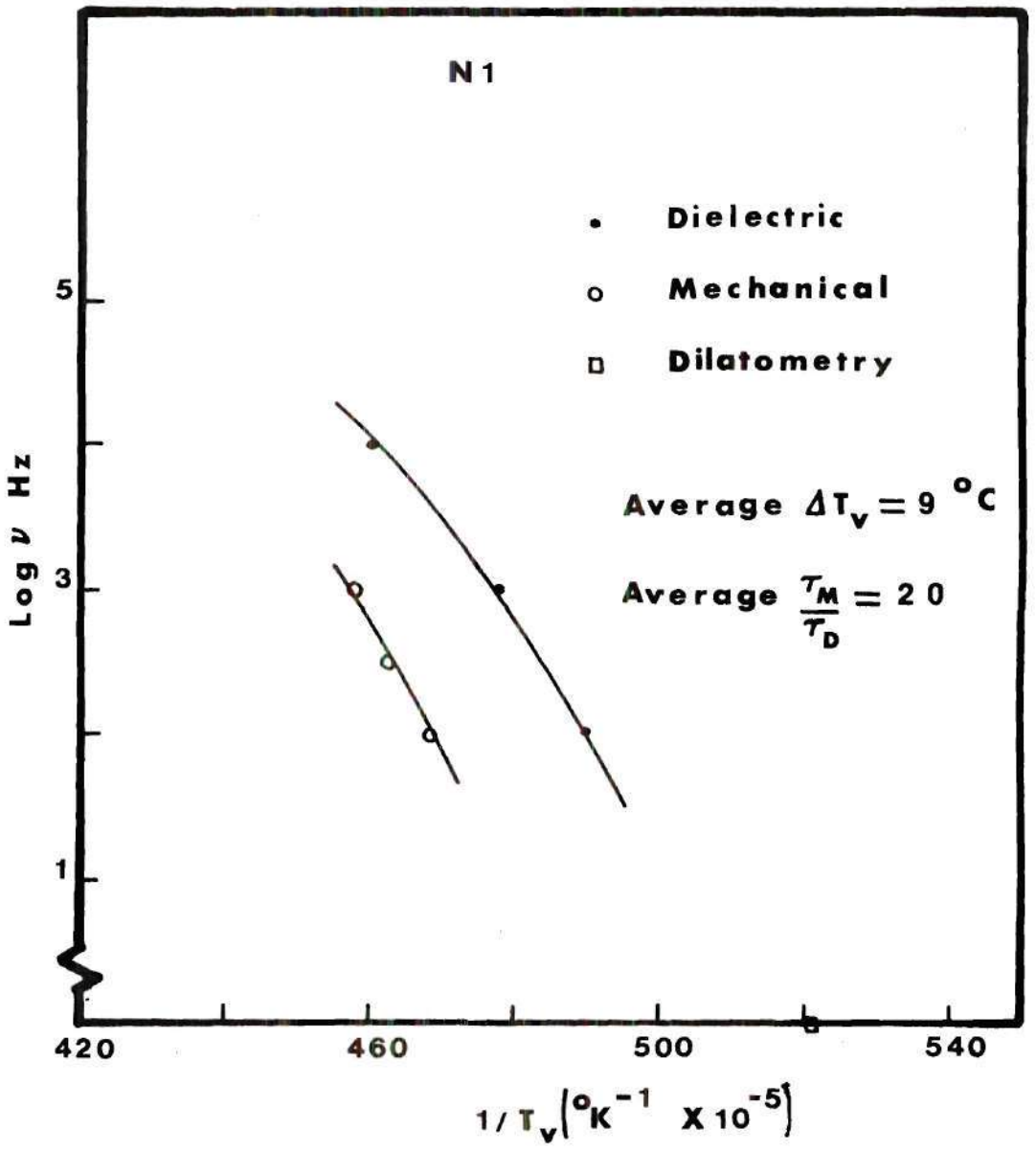

Figure 16-D. Viscoelastic Transition Curves for N1 at Atmospheric Pressure

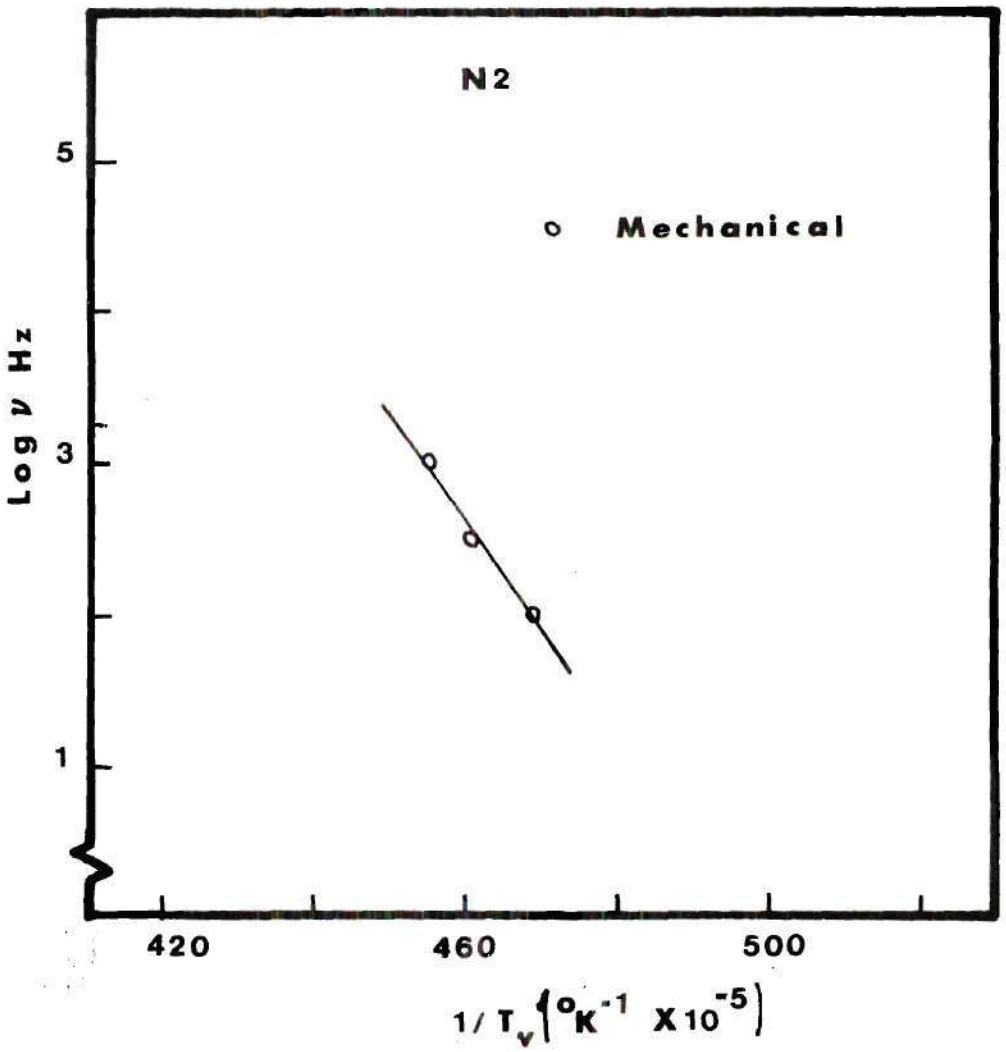

Figure 16-E. Viscoelastic Transition Curves for N2 at Atmospheric Pressure

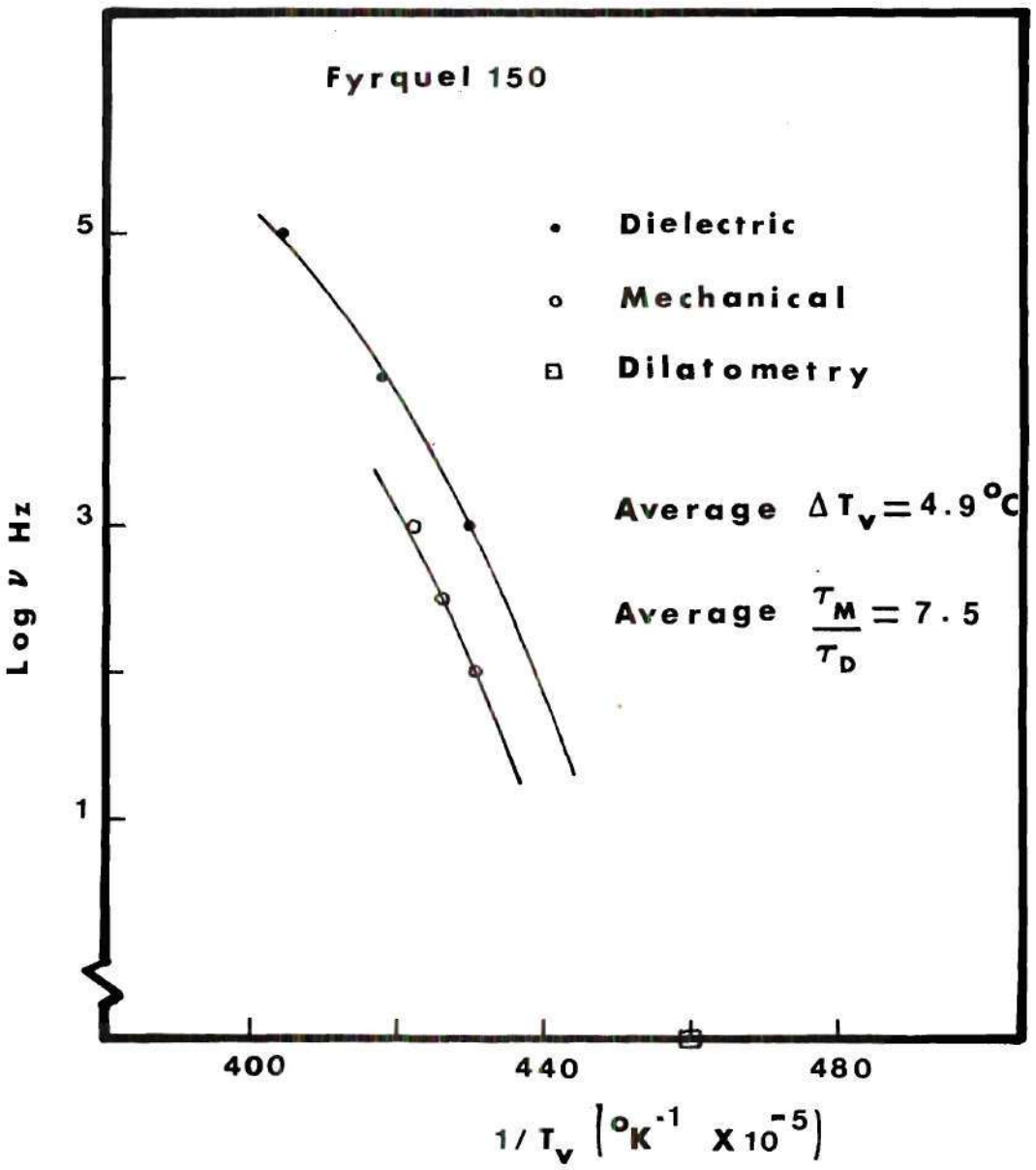

Figure 16-F. Viscoelastic Transition Curves for Fyrquel 150 at Atmospheric Pressure

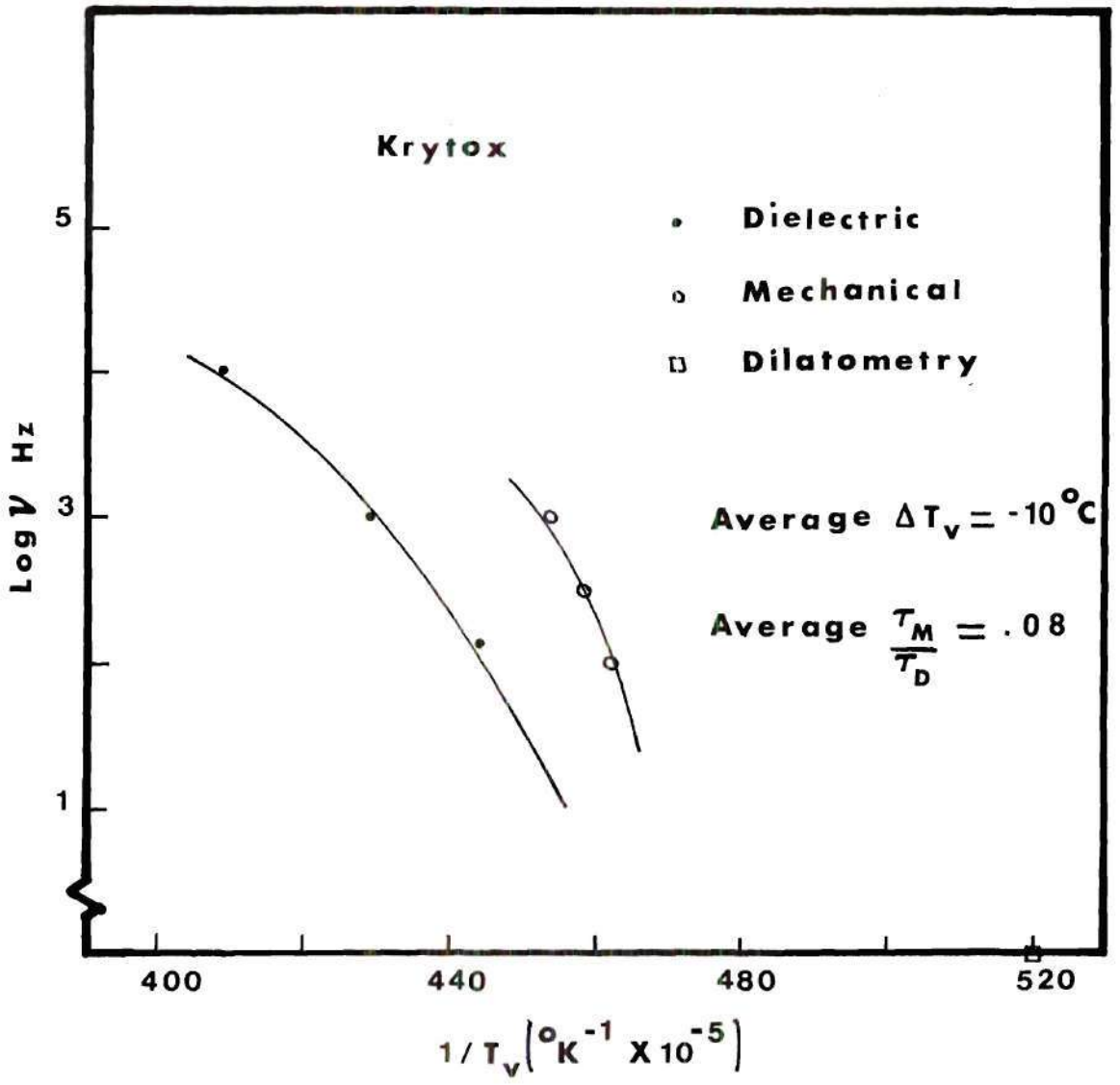

Figure 16-G. Viscoelastic Transition Curves for Krytox at Atmospheric Pressure

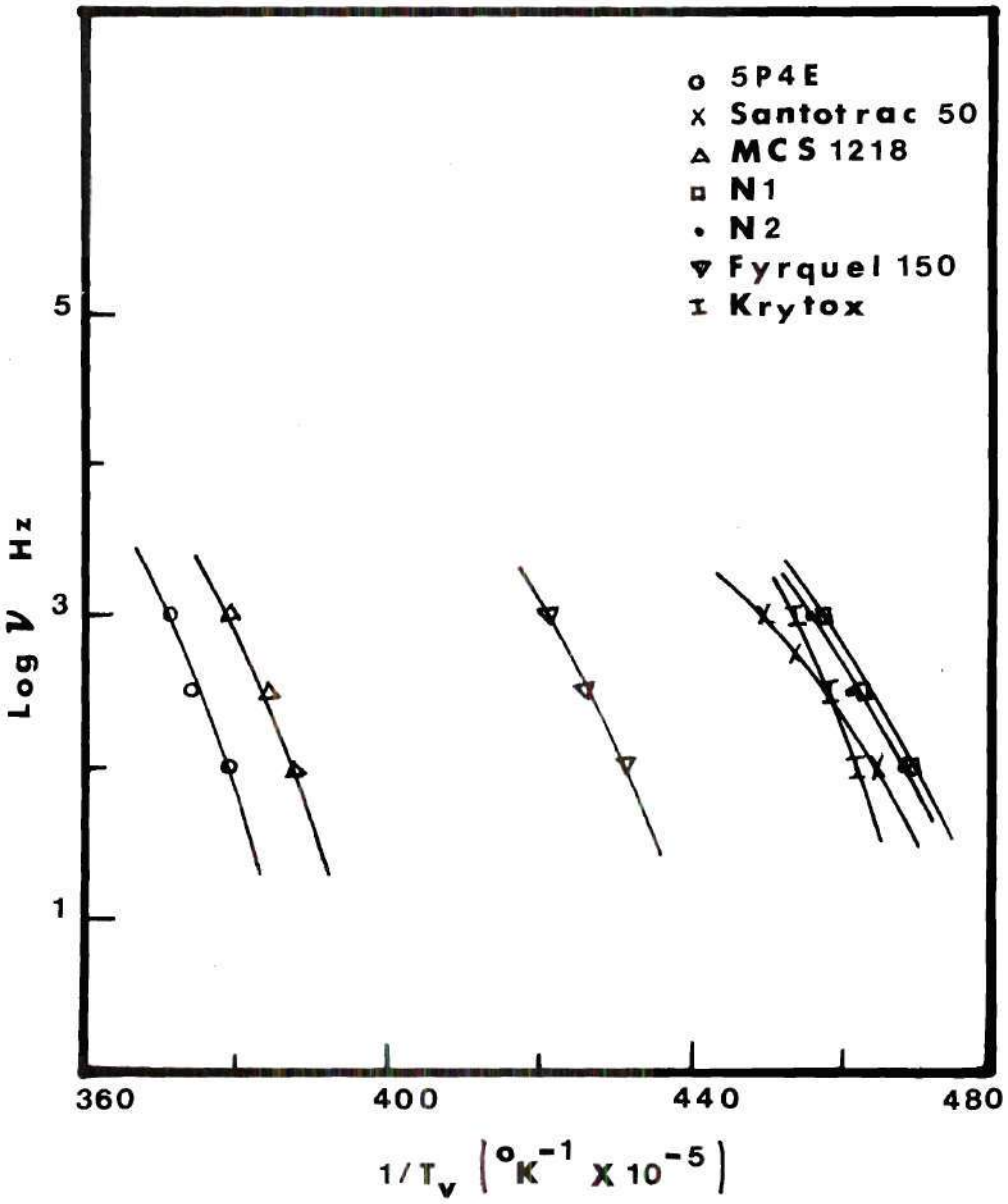

Figure 17. Viscoelastic Transition Curve of 5P4E, Santotrac 50, MCS 1218, N1, N2, Fyrquel 150 and Krytox as obtained by Shear Mechanical Measurements

CHAPTER V

DISCUSSION OF RESULTS

A. Viscoelastic Transition Behavior of the Experimental Liquids

For viscoelastic liquids, at high temperature, the storage modulus has a very small value. The storage modulus approaches zero with increasing temperature. Macroscopically, this means that the phase angle between stress and strain approaches 90 degrees as the stored energy per cycle of deformation becomes negligible compared with that dissipated as heat [13]. It is in the transition zone between glasslike and liquidlike consistency that the dependence of the storage modulus on temperature is most pronounced. Below the viscoelastic transition temperature, the configurations of lubricant chain backbones are largely immobilized and the large changes in viscoelastic properties with temperature which occur in the transition zone do not appear (See Figure 15).

This behavior can be understood qualitatively on the basis that the retardation and relaxation times which constitute the viscoelastic spectra increase rapidly with decreasing temperature (See Figure 16). At high temperatures, before transition, $\omega\tau_M$ is much less than unity. Therefore, all configurational modes of motion within entanglement coupling points can freely occur [13]. In the transition zone, $\omega\tau_M$ is of the order of one and at the viscoelastic transition temperature, $\omega\tau_M$ is equal to one. But at low temperatures, where $\omega\tau_M \gg 1$, practically no configurational changes occur within the period of deformation for

the strain amplitudes encountered in these experiments.

A comparison between the viscoelastic transition behavior of the experimental liquids indicates the following trends:

1. In the frequency range covered, the viscoelastic transition temperature of 5P4E was found to be highest and that of N1 was found to be lowest (-4 C and -55.2 C respectively) at 1000 Hz, MCS 1218 also has a high viscoelastic transition temperature (-10 C at 1000 Hz), very near to that of 5P4E. Santotrac 50, Krytox and N2 have viscoelastic transition temperature (-50.8 C, -53 C, -53.5 C respectively at 1000 Hz) which are very near to that of N1. The viscoelastic transition temperature of Fyrquel 150 (-36.75 C at 1000 Hz) falls in the middle of the viscoelastic transition temperatures of 5P4E and N1.

2. T_v increases with frequency. The rate of increase of T_v with frequency was found to be lowest for Krytox (4 C per decade change in frequency, and highest for Santotrac 50 (7.2 C per decade change in frequency). Fyrquel 150 and N1 have also low rates of increase of T_v with frequency (4.25 and 4.55 C per decade change in frequency respectively). On the other hand, N2 and MCS 1218 have high rate of increase of T_v with frequency (6.5 C per decade change in frequency). On an average, viscoelastic transition temperature increased by 5.5 C per decade change in frequency.

3. The viscoelastic transition temperature of the naphthenic base oil blended with four percent high molecular weight polymer was found to be only a little higher than that of the base oil (-53.5 and -55.2 C at 1000 Hz respectively). The rate of increase of T_v with frequency for N2 was also found to be higher than that of N1 (6.5 and

4.55 C per decade change in frequency respectively). These effects can be explained by the fact that the viscoelastic transition in polymers occurs at high temperatures compared to those of lubricating oils and also the rate of increase of T_v with frequency for polymers is approximately 7 C per decade change in frequency [59].

B. Comparison of Shear Mechanical Data with Dilatometry and Dielectric Measurements

It should be emphasized that a close correspondence among mechanical, dielectric and volume relaxations can not be expected [11,13,14,55,60,61]. Mechanical relaxation depends on molecular motions whereas dielectric relaxation depends on orientation of electric dipoles. Although similar molecular motions may be involved, the quantities measured (such as electrical polarization) corresponding to various molecular processes may have very different relative magnitudes from that observed mechanically or may be completely absent [13]. Also, in many polar molecules, orientation of the dipole can occur without movement of the whole molecule. In such cases, the dielectric and mechanical relaxation time might be expected to be different and to have different temperature dependences [11].

The viscoelastic transition temperatures as obtained from shear mechanical measurements were found to be higher than those obtained from dielectric measurement for all the liquids studied except Krytox for which the case was reversed. The highest average temperature difference was obtained for N1 (9 C) and the lowest average temperature difference was obtained for MCS 1218 (1 C). For the other three liquids - Santotrac 50, 5P4E and Fyrquel 150, the average temperature difference was 4.9, 4.4 and

4.9 C respectively. For Krytox, the viscoelastic transition temperature as obtained from shear mechanical measurement was found to be lower than that obtained from dielectric measurement and the average temperature difference was 10 C.

Dilatometry measurements are very low rate measurements and therefore, viscoelastic transition temperature as obtained from shear mechanical measurement can not be compared directly to that obtained from a dilatometry measurement. However, by extrapolating the shear mechanical transition curve to very low frequency we can compare the results. By considering a frequency of the range 0.01 to 0.001 Hz for 5P4E, MCS 1218, Santotrac 50, N1 and Fyrquel 150, the viscoelastic transition temperature compares well with that obtained by dilatometry measurements. However, for Krytox, the viscoelastic transition temperature as obtained by extrapolation in the above mentioned frequency range is approximately $5^{o}C$ higher than that obtained by dilatometric measurements.

The average ratio of the mechanical relaxation time to the dielectric relaxation time was found to be a minimum for Krytox (0.08) and a maximum for N1 (20). For MCS 1218, this ratio was found to be very near to 1 (1.25) which indicates that data obtained from mechanical shear are very close to those obtained from dielectric measurements. For Santotrac 50, this ratio is also very small (2.3). However, for Fyrquel 150, 5P4E and N1, this ratio is high (7.5, 10 and 20 respectively) which indicates appreciable difference in data obtained from mechanical shear and dielectric measurements. No dielectric data was available for N2.

In the frequency range covered by mechanical shear measurement, the transition curve as obtained by mechanical measurements is approximately parallel to that obtained by dielectric measurements for most of the liquids studied.

CHAPTER VI

CONCLUSIONS AND RECOMMENDATIONS

Several techniques are employed for the determination of the viscoelastic transition temperature such as dilatometry, differential scanning calorimetry, thermomechanical analysis, dielectric, light scattering and shear mechanical techniques. In elastohydrodynamic lubrication, the lubricant is sheared. So of these techniques, shear mechanical technique is more relevant than other techniques as far as its application to elastohydrodynamic lubrication is concerned.

Many workers in the field of elastohydrodynamic lubrication assume that the lubricant in EHD contacts remains in the viscous liquid state. However, the viscoelastic transition temperature of many lubricants (such as -4 and -10 C at 1000 Hz for 5P4E and MCS 1218 respectively) is high even at atmospheric pressure. The viscoelastic transition temperature increases with pressure and frequency, and there exists high pressure, of the order of 0.7 GPa, at room temperature in an EHD contact. Therefore, many lubricants may be in the glassy state for a significant position of the time they are in the contact. Adjustment to the existing theory will be necessary if the physical state of a lubricating oil in an EHD contact indicates that it falls in or near the glassy state. In that case, the solid-like properties of the lubricant will be the controlling material characteristics.

The magnitudes of the strain and the rate of strain applied in shear mechanical technique are much smaller than those existing in elastohydrodynamic lubrication. In this work the average values of the magnitude of the strain and the rate of strain applied were 4.4×10^{-4} and 1.35 sec^{-1} respectively, whereas in elastohydrodynamic lubrication, the corresponding values are 10^5 and 10^8 sec^{-1} respectively. The behaviour of the liquid in elastohydrodynamic lubrication under such high values of strain and rate of strain may be different from that of the the same liquid in these experiments. Although the magnitude of the applied strain may effect the rheological behavior of the liquid, it is not expected to change the viscoelastic transition. Therefore, shear mechanical technique is a useful tool in determining the viscoelastic transition temperature of liquids.

Although a comparison was made between the dielectric data and shear relaxation data, no correlation was obtained. It appears that different mechanisms of molecular movement are involved in the dielectric and shear relaxation processes. It would seem possible, therefore, that in certain cases the study of the dielectric properties of liquids in the supercooled state may provide information which will complement the information obtained from the study of the mechanical properties. If so, the comparative ease with which dielectric measurements can be made would enable liquids to be characterized much more rapidly than by the direct determination of the shear properties.

Although in this work coaxial cylinder geometry was used, other

geometries as described before may also be used to take data to cover a wider range of applied strain and frequency. Besides this, in place of using the method of direct measurements of sinusoidally varying stress and strain, the method of measurements involving the mechanical impedance of a moving element has also been used [13].

It is difficult to use shear mechanical technique at pressures more than atmospheric pressure due to complications involved in the design and also in the measurements of the applied stress and strain. But the author feels that the data taken at higher pressures will help us to understand the behavior of the lubricant in elastohydrodynamic lubrication.

The rate of cooling is known to effect the viscoelastic transition temperature. The rate of cooling employed in these experiments was 0.25 to 0.5 C per minute. The author feels that both the dielectric and shear mechanical measurements should be taken at the same controlled rate of cooling, preferably over the same temperature, pressure, and frequency range so that definite conclusions can be drawn regarding the correlations which might be possible between the dielectric and mechanical properties.

APPENDICES

APPENDIX A

DESCRIPTION OF EXPERIMENTAL FLUIDS

The following table summarizes the oil investigated in this research and gives characteristic data for each oil.

Experimental Fluids

Symbol	Description
5P4E	Polyphenyl Ether
Santotrac 50	Synthetic Cycloaliphatic Hydrocarbon Traction Fluid
MCS 1218	Cycloaliphatic Hydrocarbon
Fyrquel 150 R & O	Tri-Aryl Phosphate
Krytox 143-AB	Perfluorinated Polymer
N1	Naphthenic Base Oil R-620-15
N2	N1 + 4% Poly Alkyl Methacrylate (PL-4521)

Fluid Characterization

Symbol: 5P4E

Type: Five-ring Polyphenyl Ether

Source: Monsanto Company

Properties:		
	Viscosity at 37.8 C, m^2/s	363×10^{-6}
	Viscosity at 98.9 C, m^2/s	13.1×10^{-6}
	Density at 22.2 C, kg/m^3	1.205×10^{3}
	Density at 37.8 C, kg/m^3	1.19×10^{3}
	Flash Point, C	288
	Pour Point, C	4.4

Symbol:	Santotrac 50	
Source:	Monsanto Company	
Type:	Synthetic Cycloaliphatic Hydrocarbon Traction Fluid	
Properties:	Viscosity at 37.8 C, m^2/s	$.34 \times 10^{-4}$
	Viscosity at 98.9 C, m^2/s	$.056 \times 10^{-4}$
	Pour Point C	-37
	Density at 37.8 C, kg/m^3	$.889 \times 10^3$
	Flash Point, C	163
	Fire Point, C	174
	Specific Heat at 37.8 C, J/Kg. K	.51
	Additive package includes: Antiwear (zinc dialkyl dithiophosphate), Oxidation inhibitor Antifoam, VI Improver (Polymethacrylate)	

Symbol:	MCS-1218	
Source:	Monsanto Company	
Type:	Cycloaliphatic Hydrocarbon	
Properties:	It is a combination of two components. Each have a molecular weight less than 1000.	
	Viscosity at 37.8 C, m^2/s	1418×10^{-6}
	Viscosity at 98.9 C, m^2/s	18.37×10^{-6}
	Density at 23.9 C, kg/m^3	0.94×10^3

Symbol:	Fyrquel 150 R & O	
Type:	Tri-Aryl Phosphate	
Source:	Stauffer Chemical Company	
Properties:	Density at 15.6 C, kg/m^3	1165
	Pour Point, C	-23
	Viscosity at 37.8 C, Ns/m^2	36.94×10^{-3}
	Viscosity at 98.9 C, Ns/m^2	4.83×10^{-3}

Symbol:	Krytox 143-AB	
Type:	Perfluorinated Polymer	
Source:	Dupont Company	
Properties:	Viscosity at 37.8 C, m^2/s	96.6×10^{-6}
	Viscosity at 98.9 C, m^2/s	11.45×10^{-6}
	Density at 24 C, kg/m^3	1890
	Density at 98.9 C, kg/m^3	1760

Symbol:	N1	
Source:	Sun Oil Company	
Type:	Naphthenic Base Oil R-620-15	
Properties:	Viscosity at 37.8 C, m^2/s	24×10^{-6}
	Viscosity at 98.9 C, m^2/s	3.728×10^{-6}
	Viscosity Index (ASTM-D-2270)	-13
	Flash Point, C	157
	Pour Point, C	-43
	Density at 20 C, kg/m^3	0.9157×10^3
	Average Molecular Weight	305

Symbol:	PL 4521, used as an additive in lubricant N1	
Source:	Rohm and Haas Company	
Type:	Polyalkylmethacrylate in oil solution	
Properties:	Percent polyalkylmethacrylate in solution	36.1
	Viscosity at 98.9 C, m^2/s	7.96×10^{-4}
	Viscosity average molecular weight	560,000
	Gel permeation chromatograph molecular weight average	828,000

APPENDIX B

IMPEDANCE HEAD SPECIFICATIONS

The impedance head used was model 8001 manufactured by Brüel and Kjaer (B and K). The general performance specifications are given below:

Accelerometer sensitivity	25 mV/N
Force gauge sensitivity	330 mV/N
Transverse sensitivity of accelerometer	< 3%
Frequency range, Hz	± 2% 1 - 7000
	± 10% 1 - 10,000
Maximum load in tension	300 N
Maximum load in compression	2000 N

REFERENCES

1. Nagaraj, H. S., "Investigation of Some Temperature-Related Phenomena in Elastohydrodynamic Contacts including Surface Roughness Effects", Ph.D. Thesis, Georgia Institute of Technology, Georgia, December 1976.

2. Fuller, Dudley D., "Theory and Practice of Lubrication for Engineers", John Wiley and Sons, New York, 1956.

3. Department of Education and Science, "Lubrication (Tribology)- A Report on the Present Position and Industry's Needs", H. M. Stationary Office, London, 1966.

4. Jost, Peter H., "Economic Impact of Tribology", Mechanical Engineering, August 1975, pp. 26-33.

5. Ling, F. F., "Socio-Economic Impacts of Tribology", Proc. Tribology Workshop, National Science Foundation, April 1974, pp. 32-64.

6. Tallian, T. E., "Elastohydrodynamic Hertzian Contacts", Mechanical Engineering, Part I, November 1971, pp. 14-18, Part 2, December 1971, pp. 17-22.

7. Wedeven, Lavern D., "What is EHD", Lubrication Engineering, 31(6), 271, 1975.

8. Alsaad, M., "Light Scattering Study of the Glass Transition and the Glassy State in Lubricating Oils", Ph.D. Thesis, Georgia Institute of Technology, Atlanta, Georgia, August 1976.

9. Reynolds, O., "On the Theory of Lubrication and its Application to Mr. Beauchamp Tower's Experiments including an Experimental Determination of the Viscosity of Olive Oil", Phil. Trans. Roy. Soc., Lond., Vol. 177, Part 1, 1886, pp. 157-234.

10. Gee, G., "The Glassy State in Polymers", Contemp. Phys., 11(4).

11. Harrison, G., The Dynamic Properties of Supercooled Liquids, Academic Press, New York, 1976.

12. Turnbull, D., Contemp. Phys., 10, 473, 1969.

13. Ferry, J. D., Viscoelastic Properties of Polymers, Wiley and Sons, Inc., New York, 1961.

14. Haward, R. N., "The Physics of Glassy Polymers", Wiley and Sons, Inc., New York, 1973.

15. Kovacs, A. J., J. Polymer. Sci., 30, 131, 1958.

16. Matsuaka, S. and Maxwell, B., J. Poly. Sci., 32, 131, 1958.

17. Mckinny, J. E. and Goldstein, M., "PVT Relationships for Liquid and Glassy Poly (Vinyl Acetate)", Journal of Research of the NBS Physics and Chemistry, 78A, 331, 1974.

18. Yourtee, J. B., and Cooper, S. L., "Properties of Densified Amorphous Polystyrene", J. Appl. Polym. Sci., 18, 897, 1974.

19. Noel, F., "Thermal Analysis of Lubricating Oils", Thermonica Act., 4, 377, 1972.

20. Great, R. J., and Turnbull, D., "Glass Transition in O-Terphenyl", J. Chem. Phys., 46(4), 1967.

21. Barrall II, E. M., Porter, R. S. and Johnson, J. F., "Heat of Transition for Some Cholesteryl Esters by Differential Scanning Calorimetry", J. Phys. Chem., 71(5), 1224, 1967.

22. Johari, G. P. and Goldstein, M., "Viscous Liquids and the Glass Transition", J. Chem. Phys., 55(a), 4245, 1971.

23. Yano, O. and Wada, Y., "Dynamic and Dielectric Relaxations of Polysterene Below the Glass Temperature", J. Polym. Sci., 9(A2), 669, 1971.

24. Rank, D. H., Kiess, E. M., and Fink, U., "Brillouin Spectra of Viscous Liquids", J. Opt. Soc. Am. 56(2), 103, 1966.

25. Pinnow, D. A., Candau, S. J., Lamacchia, I. T., and Litovitz, T. A., "Brillouin Scattering: Viscoelastic Measurements in Liquids", J. Acoust. Soc. Am., 43, 13, 1968.

26. Rank, D. H., Kiess, E. M., Fink, U., and Wiggins, T. A., J. Opt. Soc. Am., 54, 1286, 1964.

27. Cummings, H. Z. and Gammon, R. W., "Rayleigh and Brillouin Scattering in Liquids" The Landau-Placzek Ratio", J. Chem. Phys., 44(7), 2785, 1966.

28. Stevens, J. R., Jackson, D. A., and Champion, J. V., "Evidence for Ordered Regions in Poly (n-butyl) Methacrylate from Light Scattering Studies", Molecular Physics, 29(6), 1893, 1975.

29. Coakley, R. W., Mitchell, R. S., Stevens, J. R., and Hunt, J. L., "Rayleigh-Brillouin Light Scattering Studies on Atactic Polystrene", A paper presented at the American Physical Society Conference, Atlanta, Georgia, April 1976.

30. Jackson, D. A., Pentecost, H. T. A., and Powels, J. G., "Hypersonic Absorption in Amorphous Polymers by Light Scattering", Molecular Physics, 23(2), 425, 1972.

31. Romberger, A. B., Eastman, D. P., and Hunt, J. L., "Evidence for Structure in Plastic from Light Scattering", J. Chem. Phys., 51(9), 3723, 1969.

32. Work, R. N., "On the Discontinuity in the Temperature Coefficient of the Velocity of Ultra Waves in Polymeric Materials", J. Appl. Phys., 27(1), 69, 1956.

33. Mitchell, R. S., and Guillet, J. E., "Brillouin Scattering in Amorphous Polymeric Solid", J. Polymer Sci.: Polymer Phys. Ed., 12, 713, 1974.

34. Friedman, E. A., Ritger, A. J. and Andrews, R. D., "Brillouin Scattering near the Glass Transition of Polymethyl Methacrylate", J. Appl. Phys., 40(11), 4243, 1969.

35. Winer, W. O., and Sanborn, D. M., "Lubricant Rheology applied to Elastohydrodynamic Lubrication", NASA CR-2837, NASA, Washington, D.C., May 1977.

36. Nielsen, L. E., "Mechanical Properties of Polymers", Reinhold Publishing Corporation, London, 1962.

37. Smith, F. W., "Lubricant Behavior in Concentrated Contact - Some Rheological Problems", ASLE Transaction, 3, 18, 1960.

38. Johnson, K. L. and Roberts, A. D., "Observation of Viscoelastic Behaviour of an EHD Lubricant Film", Proc. Roy. Soc. Lond., A-337, 217, 1974.

39. Johnson, K. L. and Cameron, R., "Shear Behavior of Elastohydrodynamic Oil Films at High Rolling Contact Pressures", Proc. Inst. Mech. Engrs., 182, Pt. 1, 307, 1967/1968.

40. Hirst, W. and Moore, A. J., "The Elastohydrodynamic Behaviour of Polyphenyl Ether", Proc. Roy. Soc. Lond., A-344, 403, 1975.

41. Stejskal, E. D. and Cameron, A., "Optical Interferometry Study of Film Formation in Lubrication of Sliding and/or Rolling Contacts", Report No. NASA CR-120842, 1972.

42. McKinney, J. E. and Belcher, H. V., "Dynamic Compressibility of Poly (Vinyl Acetate) and its Relation to Free Volume", J. Research of the National Bureau of Standards - A. Physics and Chemistry, Vol. 67A, No. 1, 43, 1963.

43. Marvin, R. S., "The Dynamic Mechanical Properties of Polyisobutylene", Proceedings of the Second International Congress on Rheology, Academic Press, Inc., New York, 1954.

44. König, W., Mütschele, W. and Pechhold, W., "Dynamic-Mechanical Investigations on Polymers in the Frequency Region 10^{-4} Hz to 10^{2} Hz", Acustica, Vol. 22, 253, 1969/70.

45. Booij, H. C., "Influence of Superimposed Steady Shear Flow on the Dynamic Properties of Non-Newtonian Fluids", Part I and II, Rheologica Acta, Band 5, Heft 3, 1966.

46. Osaki, K., Tamura, M., Kurata, M. and Kotaka, T., "Complex Modulus of Concentrated Polymer Solutions in Steady Shear", J. Phys. Chem., Vol. 69, 12, 4183, 1965.

47. Smith, T. L., Ferry, J. D. and Schremp, F. W., "Measurements of the Mechanical Properties of Polymer Solutions by Electromagnetic Transducers", J. Appl. Phys., Vol. 20, 144, 1949.

48. Markovitz, H., Yavorsky, P. M., Harper, R. C., Zapas, L. J., and Dewitt, T. W., "Instrument for Measuring Dynamic Viscosities and Rigidities", Rev. Sci. Instr., Vol. 23, 8, 430, 1951.

49. Heijboer, J., "Study of the Movements of Cycloalkyl Side Groups in Polymethacrylates by Dynamic Mechanical Measurements", J. Poly. Sci., C, 16, 3413, 1968.

50. Nolle, A. W., "Methods for Measuring Dynamic Mechanical Properties of Rubber-like Materials", J. Appl. Phys., Vol. 19, 753, 1948.

51. Birnboim, M. H. and Ferry, J. D., "Method for Measuring Dynamic Mechanical Properties of Viscoelastic Liquids and Gels: the Gelation of Polyvinyl Chloride", J. Appl. Phys., Vol. 32, 11, 2305, 1961.

52. Date, M. and Fukada, E., "A Method for Direct Indication of Real and Imaginary Dynamic Elastic Moduli of Viscoelastic Materials", Rep. Prog. Polymer Phys. Japan, 7, 183, 1964.

53. Simmons, J. M., "A Servo-Controlled Rheometer for Measurement of the Dynamic Modulus of Viscoelastic Liquids", J. Sci. Instr., Vol. 43, 887, 1966.

54. Miles, D. O., "Sinusoidal Shear Generator for Study of Viscoelasticity", J. Appl. Phys., Vol. 33, 4, 1422, 1962.

55. McCrum, N. G., Read, B. E. and Williams, G., "An Elastic and Dielectric Effects in Polymeric Solids", John Wiley and Sons, New York, 1967.

56. Sanborn, D. M. and Winer, W. O., "Investigations of Lubricant Rheology as Applied to Elastohydrodynamic Lubrication", to be published by NASA, Washington, D.C.

57. Philippoff, W., in Physical Acoustics, edited by Mason, W. P., Vol. IIB, Academic, New Yrok, 1965, p. 1.

58. Private communication with B & K Company.

59. Nielsen, L. E., "Mechanical Properties of Polymers and Composites", Vol. 1, Marcel Decker, Inc., New York, 1974.

60. Kane, R., Litovitz, T. A., and McDuffie, "Comparison of Dielectric and Mechanical Relaxation Processes in Glycerol-n-Propanol Mixtures", J. Chem. Phys., Vol. 45, 3, 1790, 1966.

61. Glover, G. M. and Matheson, A. J., "Shear Viscoelastic Relaxation of a Nitrate Salt", Trans. Farad. Soc., 67, 1960, 1971.

62. "Instructions and Applications - Impedance Heads Type 8000 and 8001", Bruel and Kjaer, Naerum, Denmark, 1971.

63. "Instruction Manual for Model 504 Transistorized Electrostatic Charge Amplifier", Kistler Instrument Corporation, Clarence, New York, 1965.